REPORT DOCUMENTATION PAGE

Form Approved OMB NO. 0704-0188

The public reporting burden for this collection of information is estimated to average 1 hour per response, including the time for reviewing instructions, searching existing data sources, gathering and maintaining the data needed, and completing and reviewing the collection of information. Send comments regarding this burden estimate or any other aspect of this collection of information, including suggesstions for reducing this burden, to Washington Headquarters Services, Directorate for Information Operations and Reports, 1215 Jefferson Davis Highway, Suite 1204, Arlington VA, 22202-4302. Respondents should be aware that notwithstanding any other provision of law, no person shall be subject to any oenalty for failing to comply with a collection of information if it does not display a currently valid OMB control number.
PLEASE DO NOT RETURN YOUR FORM TO THE ABOVE ADDRESS.

1. REPORT DATE (DD-MM-YYYY)	2. REPORT TYPE	3. DATES COVERED (From - To)
22-04-2014	Final Report	1-Jul-2010 - 31-Jan-2014

4. TITLE AND SUBTITLE
Final Report: Accounting for Hydrologic State in Ground-Penetrating Radar Classification Systems

5a. CONTRACT NUMBER
W911NF-10-1-0292

5b. GRANT NUMBER

5c. PROGRAM ELEMENT NUMBER
611102

6. AUTHORS
Stephen Moysey

5d. PROJECT NUMBER

5e. TASK NUMBER

5f. WORK UNIT NUMBER

7. PERFORMING ORGANIZATION NAMES AND ADDRESSES
Clemson University
300 Brackett Hall
Box 345702
Clemson, SC 29634 -5702

8. PERFORMING ORGANIZATION REPORT NUMBER

9. SPONSORING/MONITORING AGENCY NAME(S) AND ADDRESS (ES)
U.S. Army Research Office
P.O. Box 12211
Research Triangle Park, NC 27709-2211

10. SPONSOR/MONITOR'S ACRONYM(S)
ARO

11. SPONSOR/MONITOR'S REPORT NUMBER(S)
57224-EV.7

12. DISTRIBUTION AVAILIBILITY STATEMENT
Approved for Public Release; Distribution Unlimited

13. SUPPLEMENTARY NOTES
The views, opinions and/or findings contained in this report are those of the author(s) and should not contrued as an official Department of the Army position, policy or decision, unless so designated by other documentation.

14. ABSTRACT
The objectives of this work were to: (1) evaluate the influence of hydrologic processes (i.e., changes in soil water content) on ground-penetrating radar (GPR) signals, particularly those associated with landmines, and (2) investigate the potential for developing contextual GPR classification systems by accounting for changes in environmental state (i.e., soil water content) using hydrologic modeling. The estimation of soil water content is a major focus of this work since this property is closely related to EM wave propagation in soils (i.e., dielectric constant, electrical conductivity, wave velocity), which control radar responses. The general research hypothesis

15. SUBJECT TERMS
GPR, classification, landmine, hydrology

16. SECURITY CLASSIFICATION OF:			17. LIMITATION OF ABSTRACT	15. NUMBER OF PAGES	19a. NAME OF RESPONSIBLE PERSON
a. REPORT	b. ABSTRACT	c. THIS PAGE			Stephen Moysey
UU	UU	UU	UU		19b. TELEPHONE NUMBER 864-656-5019

Standard Form 298 (Rev 8/98)
Prescribed by ANSI Std. Z39.18

Report Title

Final Report: Accounting for Hydrologic State in Ground-Penetrating Radar Classification Systems

ABSTRACT

The objectives of this work were to: (1) evaluate the influence of hydrologic processes (i.e., changes in soil water content) on ground-penetrating radar (GPR) signals, particularly those associated with landmines, and (2) investigate the potential for developing contextual GPR classification systems by accounting for changes in environmental state (i.e., soil water content) using hydrologic modeling. The estimation of soil water content is a major focus of this work since this property is closely related to EM wave propagation in soils (i.e., dielectric constant, electrical conductivity, wave velocity), which control radar responses. The general research hypothesis guiding this work is that accounting for hydrologic state in classification systems will allow for improved generalization of landmine classification tools to a broader range of sites under varying operational conditions. The focus of the research was on two-dimensional imaging and simulation, though we also demonstrated the value of three-dimensional GPR imaging for improved object detection and characterization of flow processes in soils and around buried objects like landmines. Overall we found that accurate estimates of water content can be derived from GPR signals and that accounting for the water content of a soil within a contextual classification system is likely to improve classification results.

Enter List of papers submitted or published that acknowledge ARO support from the start of the project to the date of this printing. List the papers, including journal references, in the following categories:

(a) Papers published in peer-reviewed journals (N/A for none)

Received		Paper
09/14/2012	3.00	S. M. J. Moysey, J. C. Ryan, J. A. Tarbutton, A. R. Mangel. Multi-offset ground-penetrating radar imaging of a lab-scale infiltration test, Hydrology and Earth System Sciences, (11 2011): 10095. doi: 10.5194/hessd-8-10095-2011
TOTAL:	**1**	

Number of Papers published in peer-reviewed journals:

(b) Papers published in non-peer-reviewed journals (N/A for none)

Received		Paper
TOTAL:		

Number of Papers published in non peer-reviewed journals:

(c) Presentations

Mangel, A.R., S.M. Moysey, "The use of contextual data in artificial neural network target classification algorithms for GPR data", 22nd Annual David S. Snipes/Clemson Hydrogeology Symposium, Clemson, SC, April 2014

Mangel, A. R., Moysey, S. M. J., Creighton, A., Song, Y., "Time-lapse 3D GPR imaging of a lab-scale forced infiltration experiment", 21st Annual David S. Snipes/Clemson Hydrogeology Symposium, Clemson, SC, April 2013

Creighton, A., A. Mangel, and S.M. Moysey, "Three-dimensional time-lapse infiltration monitoring using multi-channel ground penetrating radar", Geological Society of America Abstracts with Programs, Vol. 44, No. 7, p.250, 2012.

Mangel A. R., Moysey, S. M. J., Creighton, A., Smolka, A., Finley, M., "Monitoring infiltration in 3D using multi-channel ground-penetrating radar", Society of Exploration Geophysics Annual Fall Meeting, Las Vegas, Nevada, November 2012.

Mangel, A.R. S.M. Moysey, J. van der Kruk, "Time-lapse GPR WARR surveys during a lab-scale infiltration experiment, SEG-AGU Hydrogeophysics Workshop, Boise, Idaho, July 8-11 2012.

Mangel, A., S.M. Moysey, A. Creighton, A. Smolka, M. Finley, "3D multi-channel GPR imaging of a lab-scale infiltration experiment", Clemson University David Snipes Hydrogeology Symposium, Clemson, South Carolina, 2012.

Mangel A. R., Moysey, S. M. J., "AVO relationships of buried landmine surrogates in variable hydrologic conditions", The Symposium on the Application of Geophysics to Environmental and Engineering Problems (SAGEEP) hosted by The Environmental and Engineering Geophysical Society (EEGS), Tucson, Arizona, March 2012.

Moysey, S.M., "Advances in 3D soil mapping and water content estimation using multi-channel ground-penetrating radar, Abstract H44B-01 presented at 2011 Fall Meeting AGU, San Francisco, CA, Dec. 5-9, 2011, Invited Talk.

Mangel, A.R. and S.M. Moysey, "Time-lapse multi-offset imaging of infiltration in heterogeneous media", Abstract H41D-1058 presented at 2011 Fall Meeting AGU, San Francisco, CA, Dec 5-9, 2011.

Moysey, S.M., A. Mangel, "Time-lapse imaging of dynamic systems using multi-offset GPR reflection data", 12th Annual ARO Landmine and UXO Detection Meeting, Washington, D.C., 2011.

Mangel, A., S. Moysey, "Determining transient water content values with ground-penetrating radar reflection surveys", Clemson University David Snipes Hydrogeology Symposium, Clemson, South Carolina, 2011.

Mangel, A.R., and S.M. Moysey, "Time-lapse imaging of dynamic systems using multi-offset GPR reflection data, SAGEEP (Symposium on the Application of Geophysics to Environmental and Engineering Problems), Charleston, SC, April 2011.

Moysey, S.M.J. and A.R. Mangel, "Estimation of soil hydraulic properties using hydrologic trajectories in transient GPR data", Fall Meeting AGU, San Francisco, CA, Dec. 2010.

Mangel, A.R., S.M. Moysey, J.C. Ryan, J.A. Tarbutton, "Automated multi-offset ground penetrating radar data collection for monitoring lab-scale infiltration experiments", Annual Meeting SEG, Denver, CO, October 2010.

Number of Presentations: 14.00

Non Peer-Reviewed Conference Proceeding publications (other than abstracts):

Received Paper

TOTAL:

Number of Non Peer-Reviewed Conference Proceeding publications (other than abstracts):

Peer-Reviewed Conference Proceeding publications (other than abstracts):

Received		Paper
08/29/2011	2.00	Adam R. Mangel, Stephen M.J. Moysey, Jamie C. Ryan, Joshua A. Tarbutton. Automated multi-offset ground penetrating radar data collection for monitoring lab-scale infiltration experiments, 2010 SEG Technical Program Expanded Abstracts. , . : ,
09/17/2012	4.00	Adam Mangel, Stephen Moysey, Andrea Creighton, Alex Smolka, Matt Finley. Monitoring infiltration in 3D using multi-channel ground-penetrating radar, Society of Exploration Geophysics. 04-NOV-12, . : ,
TOTAL:	**2**	

Number of Peer-Reviewed Conference Proceeding publications (other than abstracts):

(d) Manuscripts

Received		Paper
02/11/2011	1.00	Adam Mangel, Stephen Moysey, Jamie Ryan, Joshua Tarbutton. Multi-offset ground-penetrating radar imaging of a lab-scale infiltration test, Journal of Applied Geophysics (02 2011)
04/22/2014	6.00	Adam Mangel, Jan van der Kruk, Stephen Moysey. The effect of capillarity on GPR wave dispersion in precipitation induced waveguides, TBD (07 2014)
TOTAL:	**2**	

Number of Manuscripts:

Books

Received		Paper
TOTAL:		

Patents Submitted

Patents Awarded

Awards

National Science Foundation CAREER Award (2012-2017)
Blaustein Fellowship, Stanford University (May, 2014)
Herbette Fellowship, University of Lausanne, Switzerland (2014, award deferred)

Graduate Students

NAME	PERCENT_SUPPORTED	Discipline
Adam Mangel	1.00	
FTE Equivalent:	**1.00**	
Total Number:	**1**	

Names of Post Doctorates

NAME	PERCENT_SUPPORTED
FTE Equivalent:	
Total Number:	

Names of Faculty Supported

NAME	PERCENT_SUPPORTED	National Academy Member
Stephen Moysey	0.08	
FTE Equivalent:	**0.08**	
Total Number:	**1**	

Names of Under Graduate students supported

NAME	PERCENT_SUPPORTED	Discipline
Andrea Creighton	0.10	Geology
FTE Equivalent:	**0.10**	
Total Number:	**1**	

Student Metrics

This section only applies to graduating undergraduates supported by this agreement in this reporting period

The number of undergraduates funded by this agreement who graduated during this period: 1.00

The number of undergraduates funded by this agreement who graduated during this period with a degree in science, mathematics, engineering, or technology fields:..... 1.00

The number of undergraduates funded by your agreement who graduated during this period and will continue to pursue a graduate or Ph.D. degree in science, mathematics, engineering, or technology fields:..... 1.00

Number of graduating undergraduates who achieved a 3.5 GPA to 4.0 (4.0 max scale):..... 1.00

Number of graduating undergraduates funded by a DoD funded Center of Excellence grant for Education, Research and Engineering:..... 0.00

The number of undergraduates funded by your agreement who graduated during this period and intend to work for the Department of Defense 0.00

The number of undergraduates funded by your agreement who graduated during this period and will receive scholarships or fellowships for further studies in science, mathematics, engineering or technology fields:..... 1.00

Names of Personnel receiving masters degrees

NAME

Total Number:

Names of personnel receiving PHDs

NAME

Total Number:

Names of other research staff

NAME PERCENT_SUPPORTED

FTE Equivalent:
Total Number:

Sub Contractors (DD882)

Inventions (DD882)

Scientific Progress

See Attachment

Technology Transfer

Final Project Report

Project #: W911NF-10-1-0292 **Proposal #:** 57224-EV
Project PI: Stephen Moysey, Clemson University
Project Start Date: July 1, 2010
Dates Covered By This Report: July 1, 2010 – Jan.31, 2014

Abstract

The objectives of this work were to: (1) evaluate the influence of hydrologic processes (i.e., changes in soil water content) on ground-penetrating radar (GPR) signals, particularly those associated with landmines, and (2) investigate the potential for developing contextual GPR classification systems by accounting for changes in environmental state (i.e., soil water content) using hydrologic modeling. The estimation of soil water content is a major focus of this work since this property is closely related to EM wave propagation in soils (i.e., dielectric constant, electrical conductivity, wave velocity), which control radar responses. The general research hypothesis guiding this work is that accounting for hydrologic state in classification systems will allow for improved generalization of landmine classification tools to a broader range of sites under varying operational conditions. The focus of the research was on two-dimensional imaging and simulation, though we also demonstrated the value of three-dimensional GPR imaging for improved object detection and characterization of flow processes in soils and around buried objects. Overall we found that accurate estimates of water content can be derived from GPR signals and that accounting for the water content of a soil within a contextual classification system is likely to improve classification results. The classification gains observed in this study were somewhat modest when comparing a contextual classifier to a non-contextual classifier that was trained over targets observed for a large set of hydrologic conditions. Both of these approaches significantly outperformed a classification strategy that first attempted to correct GPR signals observed at arbitrary conditions to a single hydrologic reference state. We are continuing to evaluate the significance of our results to scenarios representative of a broader range of conditions than those considered in this study.

Key Project Outcomes:

- Produced an advanced GPR imaging facility capable of automated three-dimensional investigation of radar responses of soils and objects (i.e., landmines, etc.) at field-scales under dynamic environmental conditions (e.g., soil moisture changes). This facility continues to be available to users beyond the closure of this project.
- Illustrated that 3D GPR imaging improves discrimination of objects with weak reflection signatures (e.g., non-metallic landmines) compared to 2D imaging.
- Demonstrated distinct characteristics for GPR signals (trace characteristics, phase-velocity spectra, and amplitude versus offset responses) associated with changes in water content as a result of infiltration processes.
- Demonstrated that effective medium approximations (one-dimensional flow and ray theory) provide reasonable approximations of a soil under non-equilibrium hydrologic conditions allowing for accurate estimation of water content.
- Developed and tested methodologies for classification of GPR signals within contextual neural networks; results produced to date suggest that applying a data reduction step prior to a contextual classifier produces the best classification results.

TABLE OF CONTENTS

Abstract ……..…… 1
1. Introduction……..…… 3
2. Development of an Automated GPR Imaging Facility……..….. 3
3. Empirical Results…….……..... 4
    a. Static GPR Imaging Studies……. 4
    b. Dynamic Imaging Studies…… 7
        i. Infiltration within a Homogenous Soil……. 7
        ii. Infiltration within a Heterogeneous Soil……...10
        iii. 3D Imaging of Infiltration in Soil……...……..14
4. Dispersion Analysis of GPR Data…….17
5. Neural Networks and Classification…….……19
    a. Neural Networks as a GPR Forward Model…….19
    b. Neural Networks for Target Classification……...20
        i. Network Topologies for Context-Based Classification……20
        ii. Neural Network Training Data Set……21
        iii. Neural Network Validation Data Sets.....23
        iv. Neural Network Performance in Validation Tests……24
6. Discussion and Conclusions…….29
7. References Cited……...30
    a. Publications and Presentations Produced by this Project…….....30

1. INTRODUCTION

This final report documents major results of the project "*Accounting for Hydrologic State in Ground-Penetrating Radar (GPR) Classification Systems*". First, a brief description of the capabilities of a new GPR imaging facility developed is the project is given. An overview of empirical data and results follows. The value of the new GPR facility is illustrated by showing how 3D GPR can be used to improve the detection of non-conductive targets having low GPR signal strengths. We then provide results illustrating how water content changes influence GPR signals over various objects using time-lapse imaging techniques. Associated with these empirical studies are evaluations of data analysis and modeling techniques for characterizing GPR responses under varying hydrologic conditions. Finally, we provide results of classification studies that investigate how different approaches to accounting for hydrologic context affect the classification of landmines from GPR data.

2. DEVELOPMENT OF AN AUTOMATED GPR IMAGING FACILITY

We have completed construction and development of a data collection system such that ultra-high resolution 3D GPR data can be collected efficiently and reliably. The system integrates a commercial PulseEkko Pro SPIDAR (OEM-NIC) (Sensors and Software) interface with an automated gantry positioning apparatus for the antennas, where both the radar and positioning are computer controlled using software written within LabView. This automated imaging system can be deployed in one of two tanks that we have built within the facility (large tank: 4m x 4m x 2m and small tank: 1.5m x 1.5m x 0.6m). These tanks were constructed to complement each other, e.g., materials in the smaller tank are changed more easily and it can thus more easily be used for near-surface imaging of small objects under different soil conditions or can serve as a pilot-scale test volume for the larger tank. A key advantage of the large tank is that reflection boundary effects associated with the tank walls are avoided, thereby providing conditions more representative of the field while maintaining a high degree of control of a laboratory environment. Both tanks can be equipped with irrigation systems and in-situ sensors for simulating and independently monitoring the effects of rainfall. Both tanks are also equipped with cell drains to monitor outflows and allow for accounting of water balances.

a) b) c)

Figure 1: Automated GPR imaging facility: a) small imaging tank, b) large imaging tank, and c) GPR antennas independently controlled by gantry system.

The facility has proven to be a substantial asset as it offers accurate, high speed 3D data collection over large regions, which is typically not possible in either field or lab settings. Currently, we are capable of collection rates on the order of 100 traces per second with the

SPIDAR interface. When coupled with our high-resolution positioning system, capable of moving at velocities up to 0.50 m/sec, we are able to collect fully 3D data at 0.5cm grid resolution in both down-track and cross-track directions over a 2 m^2 area in about 35 minutes. Furthermore, the system provides the versatility to collect data in a fully customizable way by programming arbitrary survey geometries. This automation capacity allows us to optimize surveys for acquisition speed by balancing between quickly acquired common-offset reflection images, which are used for imaging the spatial continuity of soils and objects, versus much slower multi-offset gathers, which are needed for determining EM wave velocities and other contextual information.

3. EMPIRICAL RESULTS

Over the course of this project, we have collected a considerable amount of data, some of which has substantially illuminated our understanding of the hydrology of soil systems, allowed us to evaluate modeling and data reduction approaches, and given us directions for further studies. We highlight some significant findings from our data collection illustrating the capability of GPR to detect different subsurface targets and changes associated with hydrologic stresses.

3.1 Static GPR Imaging Studies

We have performed a variety of experiments evaluating the ability of the new radar system to detect and discriminate between a variety of subsurface objects. Figure 2 shows the raw results (i.e., no processing) of a calibration test designed to evaluate the resolution and sensitivity of the radar (1000MHz) given varying contrasts in subsurface properties (i.e., electrically conductive water, non-conductive distilled water, and air). Despite weak signals in some cases (e.g., due to the low contrast between dry sand and the air-filled bottle), the experiment demonstrates that in all cases the radar system can discriminate objects between 2.5-7.5cm in size, i.e., well below the size of concern for both anti-tank and anti-personnel mines, for a wide range of electrical properties. This implies that high resolution GPR data can provide spatial detail useful for discriminating between mine and clutter objects. In this particular experiment the background sand was kept dry, so the strongest responses are observed for the water filled bottles with a contrast in the response for the conductive versus non-conductive targets. Weaker reflections are also apparent for the low-contrast scenario of an air-filled bottled embedded in the dry sand.

Figure 2: Schematic setup and GPR results for a calibration experiment for the new GPR system. Targets are nine Nalgene bottles filled with a NaCl solution, distilled water, or air (from left to right in the images) ranging in diameter between 2.5-7.5cm that were buried vertically in sand. Data were collected at 0.5cm increments in both the x and y direction and results are shown for one depth (i.e., timeslice) from the full 3D image.

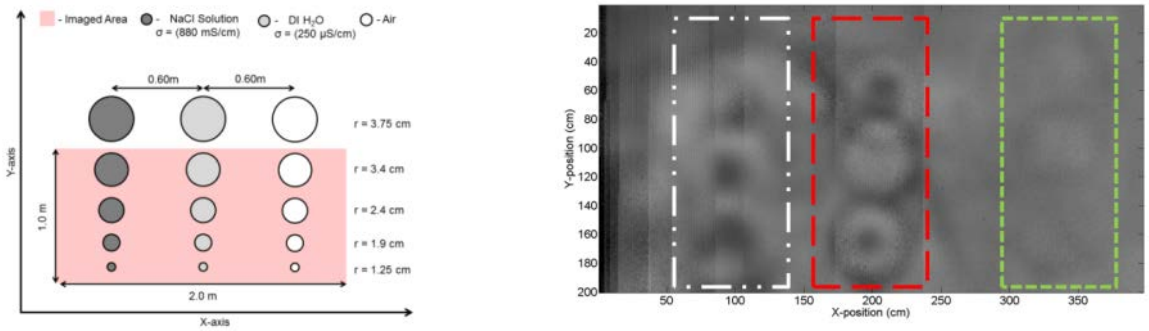

A second series of images in Figures 3-5 provide similar findings for clutter objects (a pipe and rock) versus a simulated non-metallic anti-personnel landmine. The metallic pipe is clearly identifiable with a strong response in cross-sections perpendicular to the pipe and the timeslice (Figures 3b and 3c, respectively). Though more subtle due to interference with the groundwave, the reflection is also identifiable in the cross-section parallel to the pipe (Figure 3a).

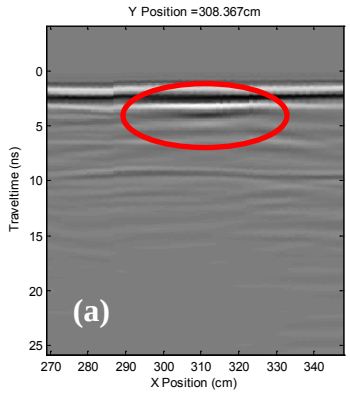

Figure 3: Cross sections obtained parallel (a) and perpendicular to an iron pipe, with a clear diffraction in the perpendicular section. The pipe is also clearly identifiable in a timeslice (c).

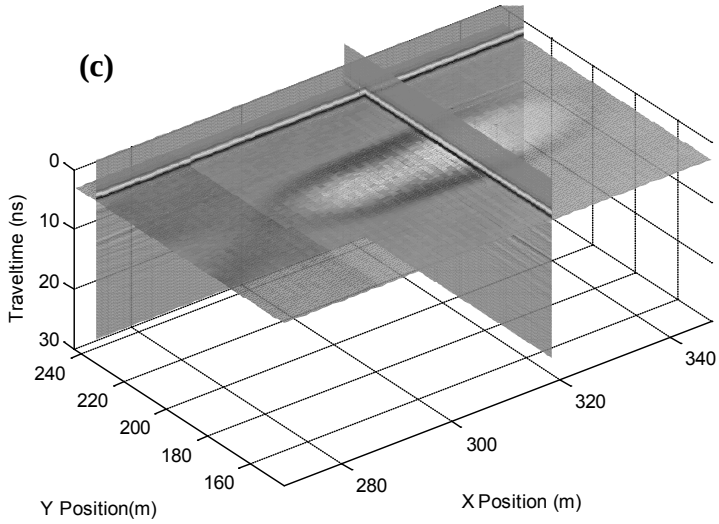

In contrast, the non-conductive rock is much more difficult to identify in the GPR data. Reflection arrivals, however, are still visible in the cross sections for this object (Figures 4a,b) and the rock is also clearly identifiable in the timeslice (Figure 4c). Figure 4d illustrates that sufficient coherent energy is reflected from the rock to define the details of its overall 3D morphology – a feature that can be important for discriminating between clutter and mine objects.

Unlike the previous two cases, results for the non-metallic landmine simulant (Figure 5) show that this object is practically undetectable in the GPR cross sections due to the low reflection strength. The mine can be identified, however, in the timeslice (Figure 5c). These results show the importance of high-resolution 3D imaging to identify and discriminate between subsurface objects with low reflection strengths, such as non-metallic landmines. Obtaining this type of data will be even more important in noisy imaging environments experienced under operational field conditions. We therefore conclude that effective utilization of 3D imaging data within subsurface classification algorithms is an important area of future research.

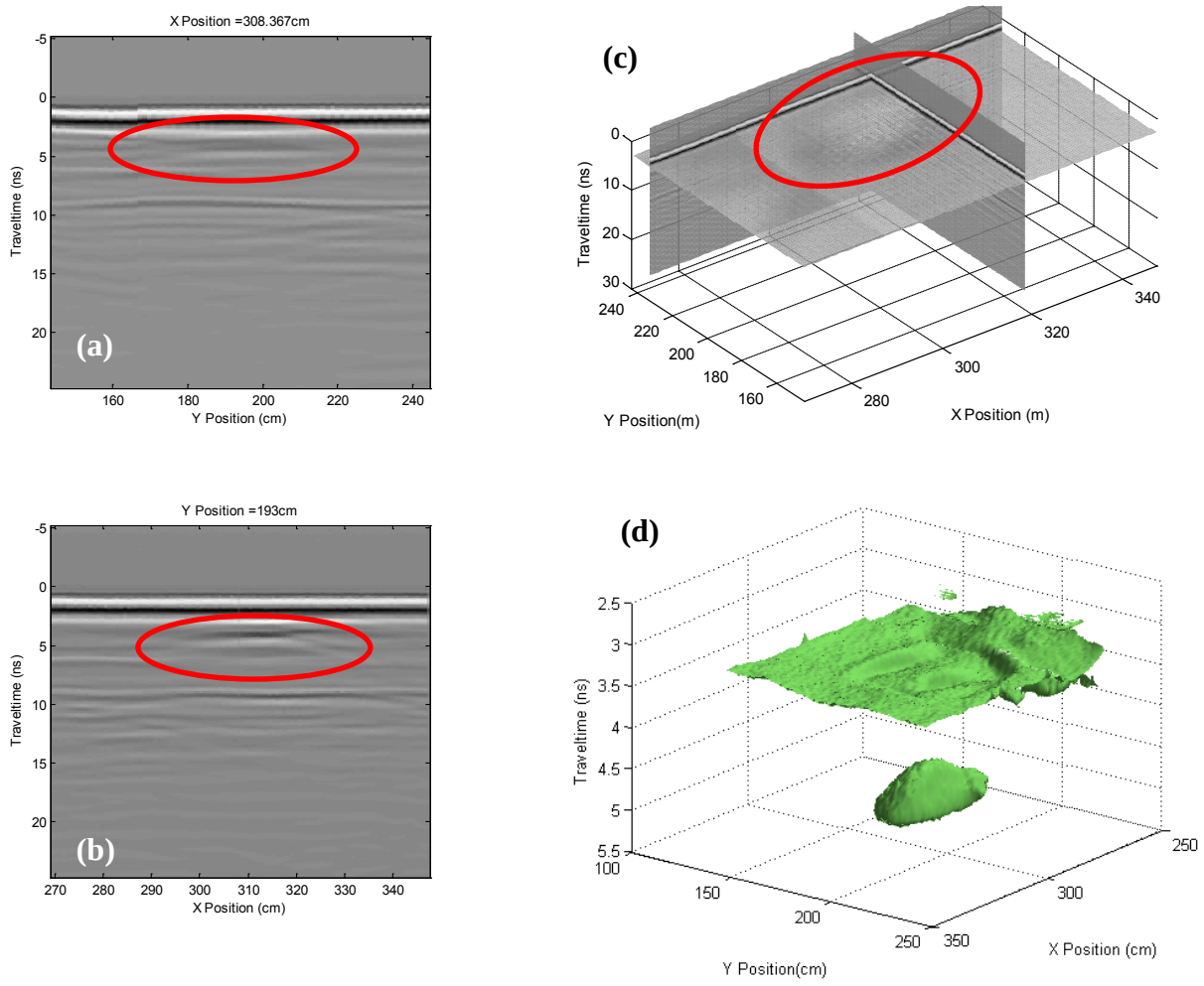

Figure 4: Orthogonal radar cross-sections obtained for the rock clutter object (a,b) showing a subtle, but clear reflection response. The outline of the object is apparent in the timeslice (c) and the overall 3D morphology of the object can be reconstructed from the high-resolution GPR data (d).

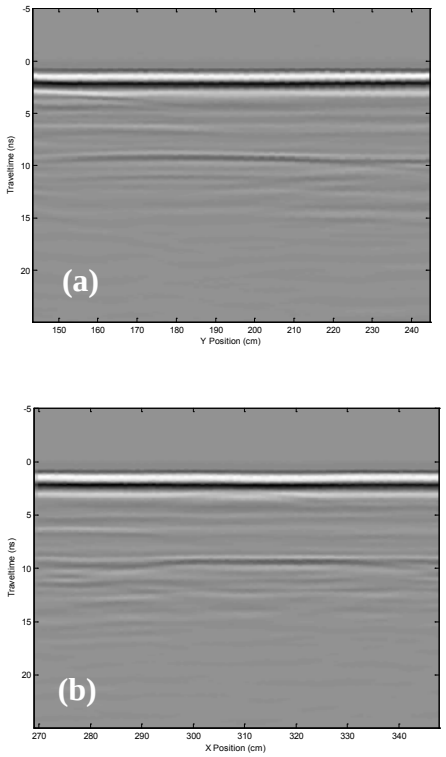

Figure 5: The GPR response of a simulated non-metallic anti-personnel landmine cannot be readily identified in either of the radar cross-sections (a,b), but can be clearly identified in the timeslice (c). The ability to more readily identify reflection objects using 3D data is particularly relevant to improving target classification results in noisy environments where profiles can be corrupted by interference from clutter objects.

3.2 Dynamic Imaging Studies: The Influence of Hydrologic State on GPR Signals

The goal of these experiments was to evaluate the influence of hydrologic processes on GPR signals. Our initial approach focused on assumptions of one-dimensional flow in soils, though GPR imaging experiments suggested the occurrence of substantial non-uniform flow. Despite this additional complication, we found that simple radar modeling techniques along with a one-dimensional flow assumption provided good estimates of water content within the soils that can be used for characterizing the hydrologic state of the soils. Additional analyses have illustrated significant potential of AVO (amplitude versus offset) analysis for discrimination of landmine signatures, while dispersion analysis may provide a means to characterize water content changes in the very near surface.

3.2.1 Infiltration within a Homogeneous Soil

Results from a 900MHz multi-offset GPR imaging experiment performed during and after a water infiltration event are shown in Figure 6. The goal of the experiment was to investigate how GPR signals changed in response to hydrologic stresses in a homogeneous porous media and to evaluate whether accurate transient estimates of the average water content could be derived from the time-lapse GPR data. Multi-offset data were collected because these measurements can be used to investigate radar responses at multiple orientations relative to targets (Figure 6a) to estimate GPR wave velocities and soil water content. The infiltration process was modeled using the software HYDRUS-1D assuming one-dimensional flow and given independently measured soil properties and the flow rates. The simulated radar response was then generated from the hydrologic simulations to provide predictions of the GPR response shown in Figure 6c.

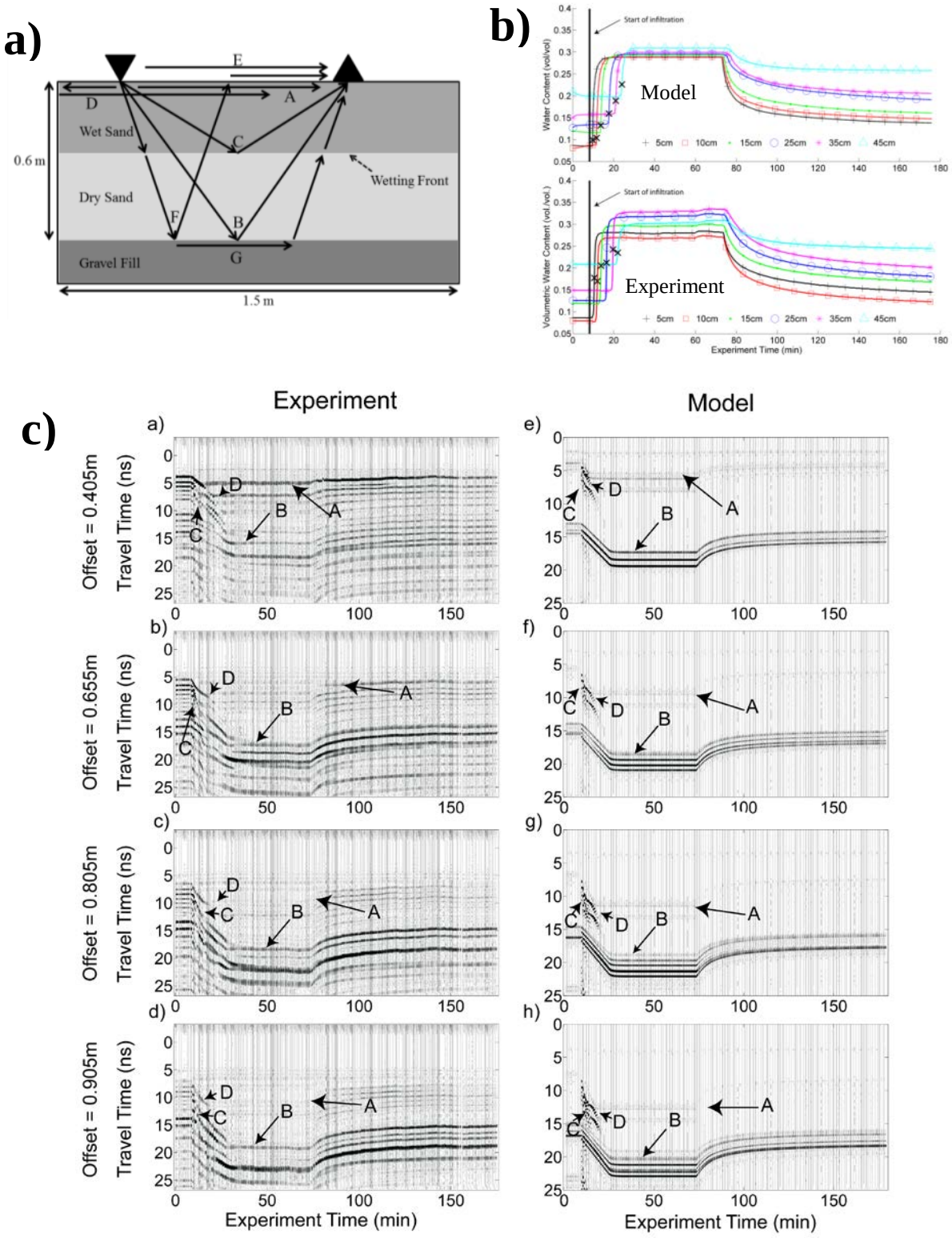

Figure 6: a) Conceptual model of flow experiment and GPR rays showing potential energy pathways through the medium, b) soil water contents measured in the experiment versus simulated by the model, c) GPR data (left) and simulation results (right) showing how multiple arrivals change over time and space in response to hydrologic influences. The models provide a good overall representation of the observed responses.

The data presented in Figure 6 shows the hydrologic and geophysical response of the experimental tank to hydrologic forcing. The measured changes in water content of the tank are directly correlated to changes in multiple arrivals on the GPR data (Figure 2c). Upon irrigation of the tank (~10 min), there is a significant change in the arrivals produced in the GPR data. This complex response led us to investigate electromagnetic wave dispersion phenomena as well as the validity of normal move-out analysis and our assumptions of 1-D flow (discussed later in this report).

The simulated GPR signals match the observed results well (Figure 6c). Some minor differences in relative amplitudes and phase relations (trace shape) occurred between the observed and simulated data sets and there was substantially more noise in the empirical dataset, partially due to scattering by the walls of the smaller tank in which the experiment was performed. Regardless, the kinematics (i.e., arrival time patterns) of the observed data are captured by the simulations across the offsets, which suggests that a normal moveout (NMO) approach to evaluating the data is appropriate.

Normal moveout (NMO) analysis is a common practice for analyzing multi-offset GPR data. Essentially, NMO provides a means to estimate wave velocities in the subsurface from multi-offset data, which also allows for translation of time-domain GPR data into the spatial domain, to provide estimates of the depth to targets. Once the wave velocity is known, the soil water content can be estimated using an appropriate petrophysical transform. We applied this analysis to the transient multi-offset GPR data collected during the homogeneous tank experiment (Figure 6) and reported the results in Mangel et al. (2012). This work demonstrated that it is possible to accurately estimate water content (Fig. 7c) and quantitatively track the depth of a hydrologic wetting front (Fig 8b) through time using this analysis. The important outcome of this result is that it demonstrated the power of simple models (one-dimensional infiltration for hydrology and ray theory for GPR) for characterizing the hydrologic state of the subsurface under arbitrary water content conditions.

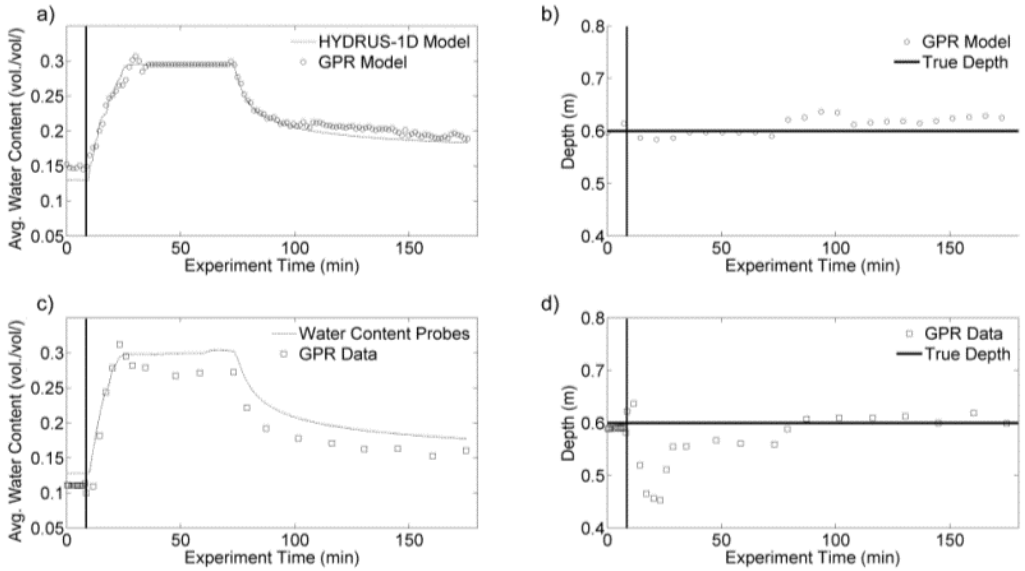

Figure 7: Comparison of water content determined from GPR versus that measured by in-situ moisture probes for (a) simulated and (e) observed data over the course of the infiltration and recovery experiment. The depth of the tank was estimated consistently for both (b) simulated and (d) observed data, except during the infiltration period when the wetting front reflection interfered with the analysis of the reflection from the bottom of the tank.

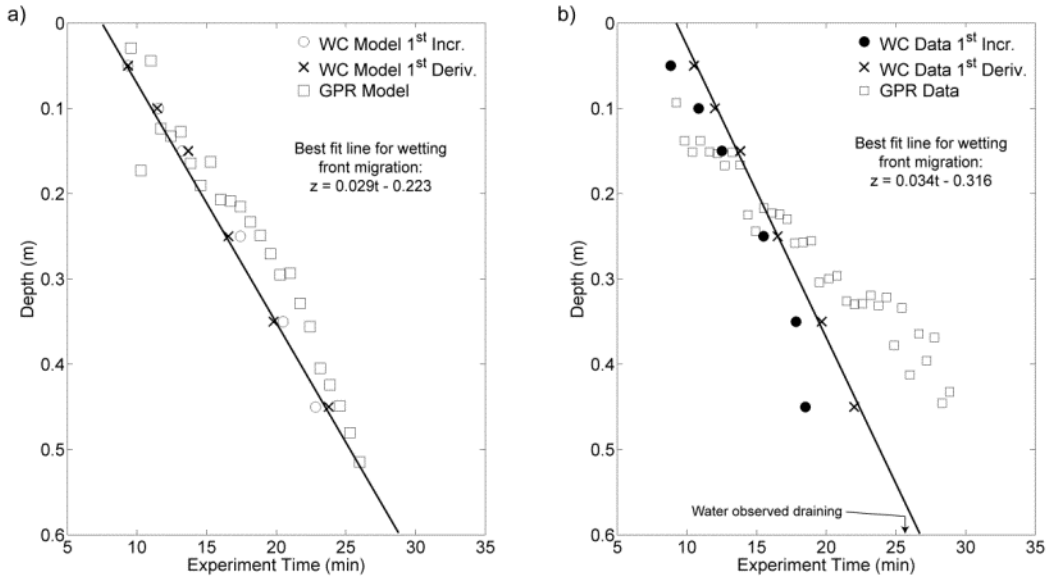

Figure 8: Estimated migration of the wetting front based on water content probe observations and analysis of the GPR data for (a) simulated and (b) observed experiments. Errors occurring when the wetting front is past 30cm depth are associated with interference from a reflection produced by the side wall of the tank.

3.2.2 Infiltration within a Heterogeneous Soils: Layers and Landmines

We performed a variety of experiments to evaluate how changes in hydrologic state affect GPR responses in heterogeneous soils. Figure 9 shows results for two specific cases: (i) a shallow subsurface soil layer, and (ii) a buried landmine surrogate. For the layer case we embedded a thin (1cm) layer of silica flour within the homogeneous sand at a depth of 15cm (Figure 9a). An anti-personnel non-metallic cylindrical (APNMC) landmine surrogate was constructed following the guidelines given by Chant et. al, (2005) and buried so the top of the mine was at a depth of 0.05 m (Fig. 9b). In both cases, water was then applied uniformly over the ground surface as the GPR data were collected in order to observe signal changes. Apart from dry soil conditions, the radar responses from the layered soil are substantially different from the landmine response (Figure 9), which was more similar to the patterns observed for the homogeneous infiltration case.

Early in the infiltration experiment (~10 min) the geophysical response of the layered soil (Fig. 9c) also closely resembles that of the homogeneous case (Fig. 6a-d) with the groundwave (A) and bottom of sand reflection (B) dominating the data. However, around 50 min elapsed time, a third reflection appears that is an indirect result of the thin layer. The layer itself is below the resolution of the radar, i.e. the radar cannot see the layer. After infiltration begins, however, water is able to build up at this interface causing a wetted zone to develop in the otherwise homogeneous upper layer, which causes the observed reflection. This was expected as the silica flour has a very low permeability compared to the sand. This interpretation is confirmed by examining the data obtained from the moisture probes embedded in the tank, which show a steep increase in water content of the upper layer while the lower layer probes never respond to the hydrologic forcing until very late in the experiment when water eventually begins to break through this impermeable layer to enter the underlying sand (Figure 10a).

The observed layered soil response is significant for two reasons. First, it demonstrates that the GPR signal obtained from a layered soil will be significantly different from that obtained from a discrete object, like a landmine. Second, it demonstrates how changes in hydrologic state can affect the apparent 'visibility' of targets due to feedbacks on environmental controls.

The hydrologic response of the landmine system was very similar to that of a homogeneous soil, i.e., a steep increase in water content was observed throughout the soil column in response to the irrigation. This hydrologic similarity therefore resulted in similar patterns observed in the GPR data for the homogeneous soil and the soil with an embedded landmine (Figure 6 vs. Figure 9d). It is therefore not possible to easily discriminate the landmine responses from a homogeneous soil response based only on data obtained with a single fixed separation distance between the antennas (i.e., antenna offset). We therefore performed further analysis of these data using amplitude versus offset (AVO) techniques and by performing high-resolution 3D imaging experiments.

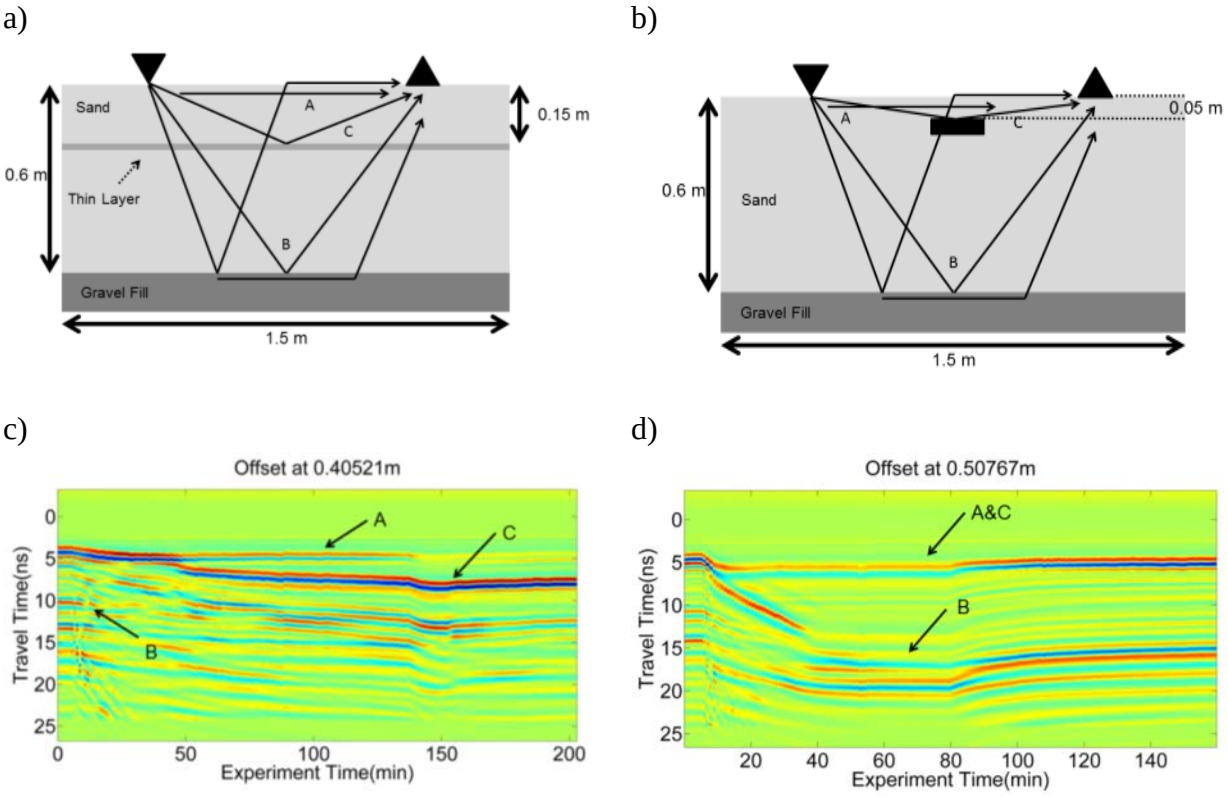

Figure 9: Conceptual diagrams of ray paths expected for different GPR arrivals from a layered soil (a) and embedded landmine (b). Flow restrictions caused by the layer have a major impact on the observed GPR signals (c), whereas the landmine signal is qualitatively similar to a homogeneous soil.

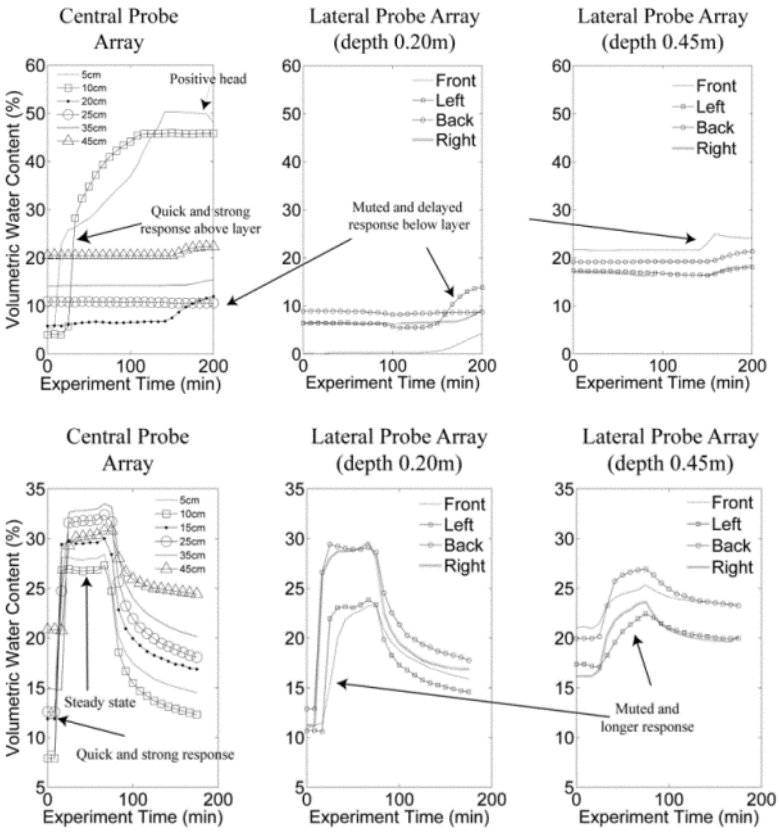

Figure 10: Comparison of water content changes observed for the layered soil (upper figures) versus a buried landmine (lower figures) during an infiltration event. The influence of the layer as a hydrologic barrier is clear, whereas the landmine responds in a manner similar to a homogeneous soil.

Results from probes placed at six depths in the center of the flow field to evaluate infiltration patterns are shown in the figures on the extreme left. Results from lateral probes placed at two depths surrounding the flow field to evaluate the influence of non-uniform flow on the results are shown in the figures in the center and right.

Complex wave interactions with buried targets can be captured by considering how the amplitude of reflections is impacted by changes in the angle of incidence of the incoming wave, i.e., through amplitude versus offset (AVO) analysis. In the landmine experiment, the data shows substantial interference between the landmine reflection and the groundwave arrivals, making it difficult to isolate the landmine signal and discriminate the presence of a landmine from the GPR data (Figure 6 vs. Figure 9d). A comparison of AVO responses in Figure 11, however, shows a distinct signature for the landmine that is not observed in the data for the homogeneous soil. The effect is particularly strong during the infiltration and recovery phase of the experiment, when the impermeable landmine has a significant impact on the overall distribution of water around it.

In a related experiment, we performed central midpoint (CMP) surveys where the transmitter and receiver antennas were centered on the landmine and the water content was controlled by sequential additions of water to the tank. In this case there is again a clear AVO response shown in Figure 12. The shape of the AVO response appears to be independent of water content in this set of experiments, suggesting that AVO could be an invariant feature of GPR signals that is valuable for detecting landmines in changing environments; note that the water content shown is for a moisture probe above the landmine simulant and that the probes below the mine showed no response. These results were reported by Mangel et al. (2012b).

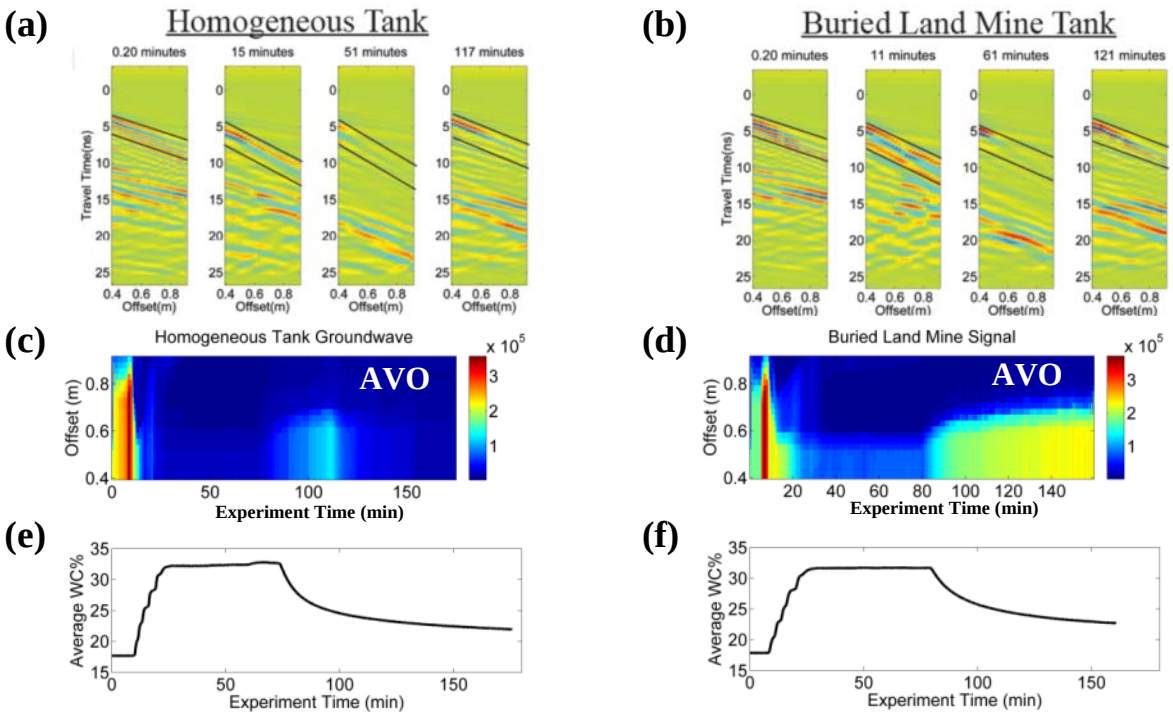

Figure 11: Typical multi-offset profiles at various times during the infiltration and recovery experiment for a homogenous tank (a) and a tank containing a landmine surrogate (b). The AVO response shows a clear difference for the soil without a landmine (c) compared to the soil containing a landmine (d). The average tank water content through each experiment (e, f).

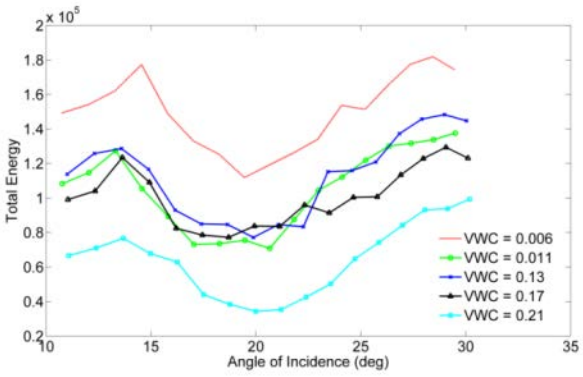

Figure 12: AVO response of a landmine under variable water content conditions determined from central midpoint (CMP) surveys. The consistent shape between the curves suggests that the AVO response may be insensitive to changes in water content.

3.2.3 Three-Dimensional Imaging of Infiltration in Soils

We have performed a variety of three-dimensional imaging experiments to improve our understanding of water flow in soils, how this is affected by the presence of landmines, and the resulting impacts on GPR signals. Our initial experiments were conducted using a multi-channel PE Pro radar purchased on a previous DURIP (57714EVRIP) project before our current GPR facility was completed. The system has 8 channels allowing for 16 different source-receiver antenna combinations and 7 parallel scans of the tank at the same offset (i.e., B scans). At each survey time during the experiment, two interleaved scans were performed to allow for 14 parallel lines to be collected. The experiment was conducted with an antenna frequency of 500 MHz. Results of the experiment are shown below in Figure 13. These data clearly show the migration of the wetting front through the tank, but also suggest the occurrence of lateral variability in the flow system. For example, the dipping reflection produced by the wetting front and irregularities across it in the GPR profile in Figure 13b (center of image), indicates that the front is not uniformly distributed in the infiltration zone. Flow is instead faster on one side of the tank than the other and the discontinuities suggest a non-uniform front, possibly due to fingering phenomena. Accounting for this type of three dimensional variability of flow is important for understanding how scattering caused by non-uniform water content distributions in the subsurface affect pattern recognition systems and our ability to constrain soil parameters needed for environmental calibration of detection algorithms. The limited resolution of the surveys in this case prevented detailed analysis of flow processes.

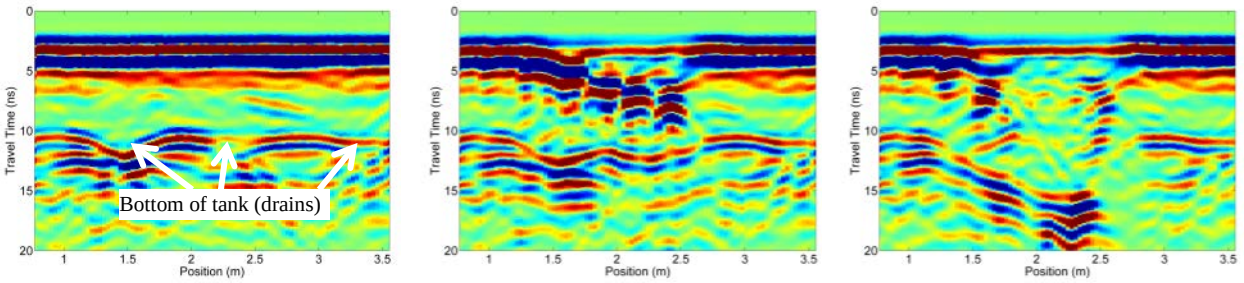

(a) Initial Conditions (b) 30 min. into infiltration (c) 2 hours into infiltration

(d)

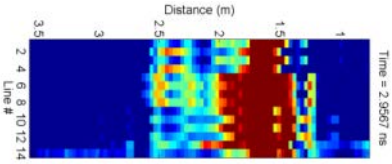

Figure 13: Results of 3D imaging of an infiltration test. Upper images show GPR cross sections illustrating the migration of the wetting front and impact on the traveltime of the bottom of tank reflection (a-c). Time slice of the GPR data showing the distribution of amplitudes across the tank at an approximately constant depth (d). The shift in colors across the tank represents a shift in GPR traveltimes, illustrating variability in flow conditions.

Upon completion of the GPR imaging facility, we are now able to produce detailed images of the subsurface at an ultra-high resolution. For example, a comparison between the non-uniformly wetted area at the top of the sand tank below where an oval irrigation grid was temporarily laid down and the response imaged by GPR is shown in Figure 14. A qualitative comparison of the images reveals that the new radar system is able to capture subtle variations in water content at a very high resolution, i.e., approximately centimeter scale. The contrast in resolution is striking when comparing results obtained during a water infiltration test monitored with the new system versus those in Figure 13, despite the fact that the latter data were collected with a cutting-edge multichannel system.

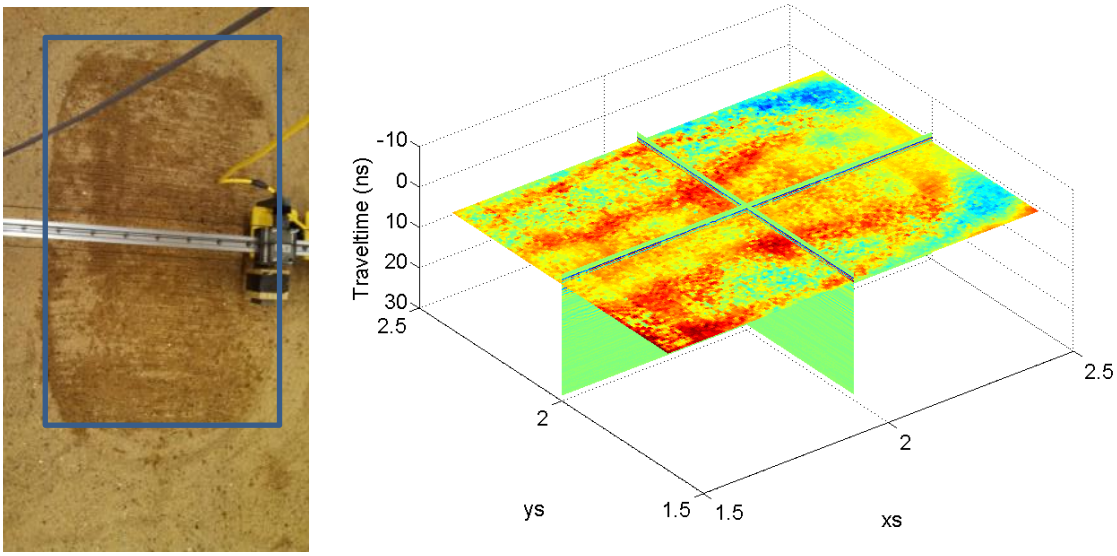

Figure 14: (left) A photo qualitatively showing variations in water content at the soil surface. (right) The radar response illustrating the potential to capture these water content variations at a very high (~cm) resolution. The outlined area in the photo indicates the approximate region shown in the GPR data.

As discussed earlier, understanding the details of flow processes and how these are impacted by buried objects (i.e., landmines) is an important task for improved interpretation of GPR data for detection and classification problems. In section 2.3.1 of this report, we demonstrated that there is little apparent difference between GPR responses produced over heterogeneous soil versus that containing a landmine. To investigate this issue more closely, we performed a time-lapse three-dimensional imaging experiment over a 30cm x 30cm area as water was allowed to drip onto the soil surface above the landmine buried at 6.5cm depth (Figure 15). Our goal was to understand how flow occurred around the mine and how this impacted GPR responses.

Figure 15: Geometry of the 3D imaging experiment of flow over a buried landmine. Drip irrigation at a point allowed water to flow around the mine.

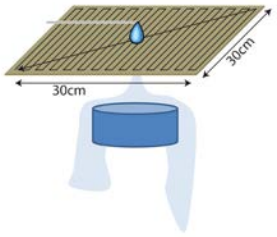

Changes in the GPR signal caused by the infiltration are clearly seen in the vertical tank profiles shown in Figure 16a, though flow in and out of the imaging plane make it difficult to reconstruct the details of flow phenomena. It is more apparent from time slices (Figure 16b), that water flow over and around the landmine is non-uniform and changes through time. Full 3D imaging surveys were collected every 1.1 minutes over the course of a 75 minute monitoring experiment. For each of these times it is possible to process the GPR data to produce a 3D isosurface image that captures the spatial continuity of reflections throughout the imaging volume, thus providing insights to flow phenomena. Water accumulation on the mine and shifts in discharge on either side of the mine are apparent in three-dimensional isosurface shown in Figure 17. While additional processing (e.g., migration) may improve images somewhat, this example clearly demonstrates the potential of radar for understanding the dynamics of in-situ flow processes. Likewise, characterizing these processes can in turn aid in the interpretation of GPR signals.

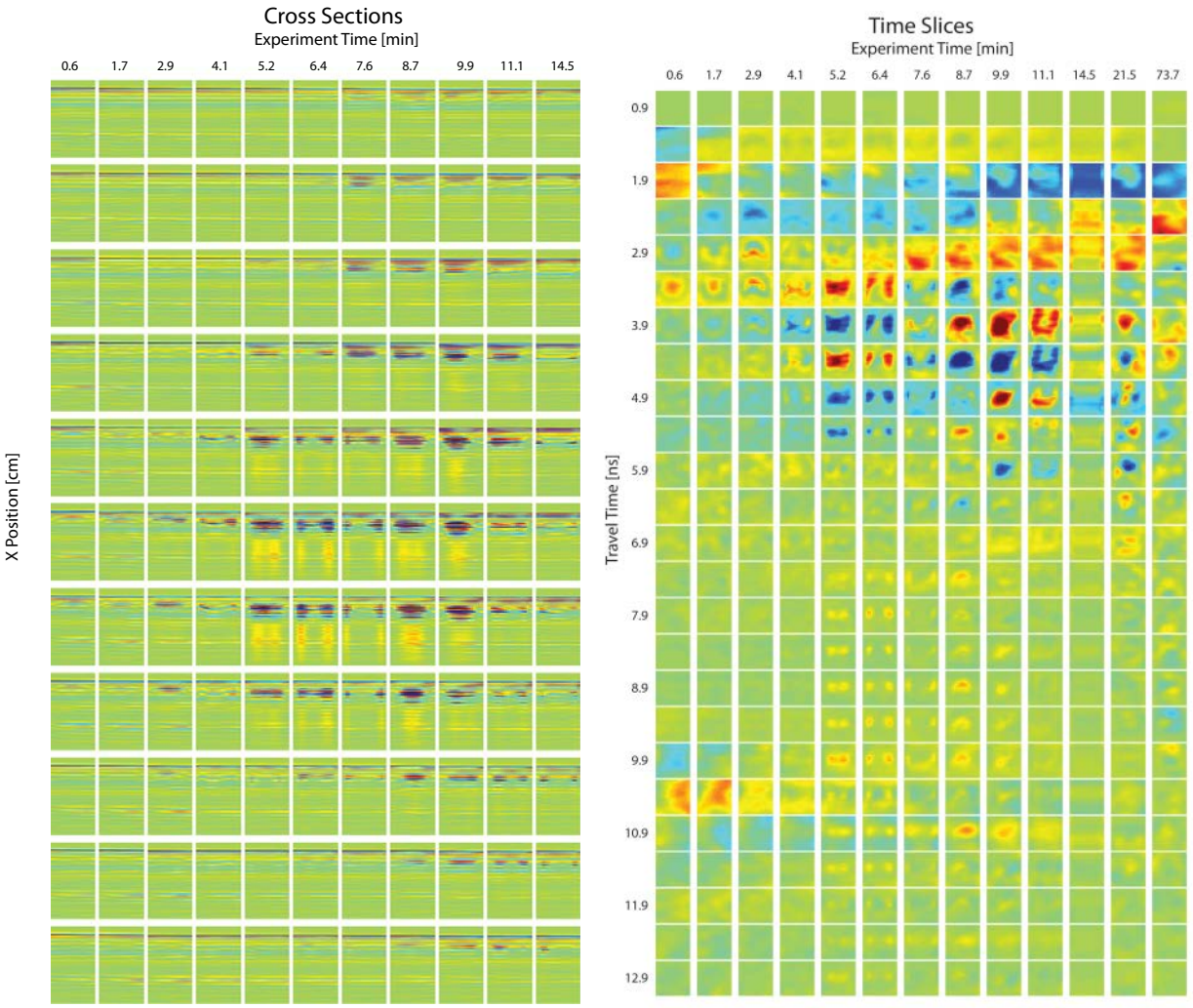

Figure 16: Reflection profiles (left) and timesclices (right) obtained during a 3D infiltration imaging experiment above a landmine. Moving across the columns provides images collected at different times in both datasets, whereas moving down a column represents slicing through the data block as vertical profiles or timeslices.

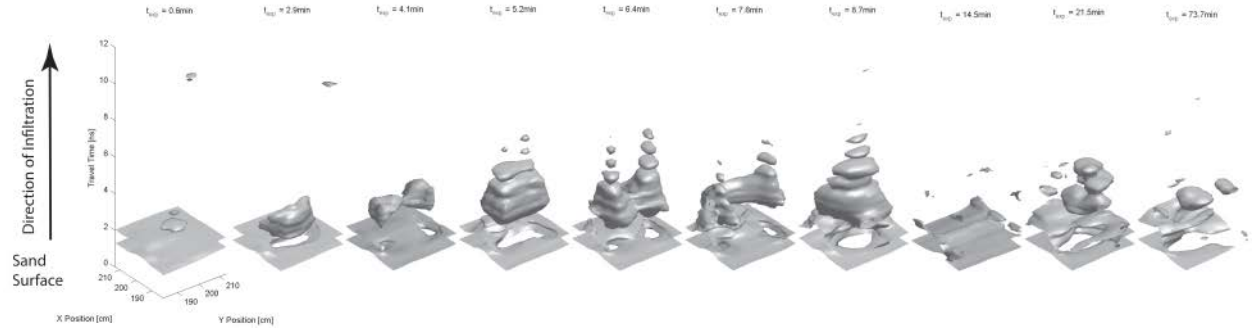

Figure 17: Isosurface images derived from GPR data showing the 3D evolution of infiltration around the mine over time. Shifts in flow occurring around alternate sides of the mine at different times are apparent. This behavior is in contrast to expectations.

1. DISPERSION ANALYSIS OF GPR DATA

When rainfall drives soil water infiltration to produce a near-surface wetted zone of a thickness similar to radar wavelengths, the wetted layer can act as a waveguide that results in the dispersion of radar waves. This problem inhibited our ability to analyze near-surface groundwave data in an article previously published as a part of this project (Mangel et al., 2012a). When the waveguide is truly a layer, however, past work has shown that it is possible to use the phase velocity spectrum of the data to characterize the geometric and dielectric properties of the wetted layer. This result has significant implications for our project given that understanding the environmental context of a landmine is critical for adaptive classification problems. The problem with the existing prior analyses, however, is that they assumed a sharp boundary between the wetted zone caused by storm water infiltration and the dry zone beneath. In reality, the shape and sharpness of this boundary is controlled by the physical properties of the soil (Figure 18), i.e., the grain size distribution which controls capillary effects in the soil.

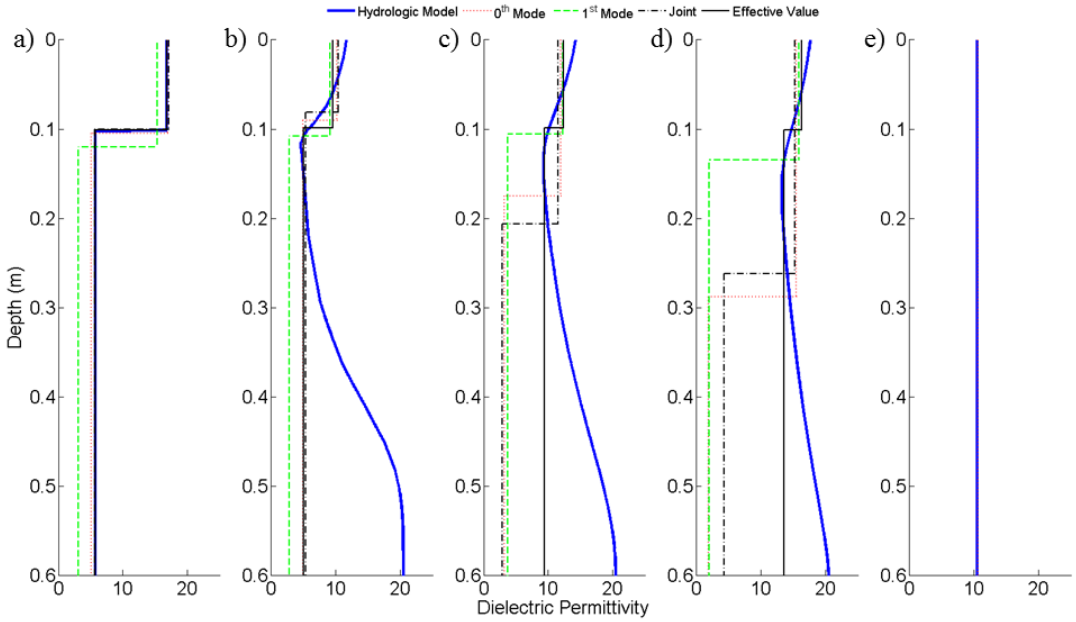

Figure 18: Permittivity profiles from the simulations showing the true hydrologic model profile (blue line), effective hydrologic model profile for a two-layer medium with the boundary defined by the maximum GPR reflection coefficient, and results of zero mode (dashed red line), first mode (dashed green line), and joint zero/first mode inversions (dashed black line) of a layered medium. Figures are shown for five different soil cases: a) infiltration occurring as a sharp front, b) low capillarity soil, n = 4.0, c) moderate capillarity soil, n = 2.1, d) high capillarity soil, n = 1.5, and e) no infiltration (i.e., no waveguide). As capillarity increase, the dispersion inversion method produces increasingly inconsistent results for the soil.

To investigate the influence of soil type on the dispersion analysis, we used coupled hydrologic and GPR forward models to simulate the effects of wave dispersion in a variety of soil types. We test the hypotheses that the number of dispersive modes will decrease as the capillary effect of a porous media increased, effectively making it more difficult to characterize the subsurface properties of the near-surface soil environment. Capillarity of the porous media was controlled using the *n*-variable of the Mualem-van Genuchten soil model, which is usually associated with grain size distribution.

We demonstrate that the dispersion of GPR waves is strongly dependent on soil specific water content profiles of a precipitation induced waveguide (Figure 19). We found that as the sharpness of the lower boundary of the dispersive waveguide decreases, the number of dispersive modes in the GPR data decreases due to the reduction in dielectric contrast causing an increase in the critical angle, which must be reached for dispersion to occur. We are still investigating the effect of capillarity on the dispersion of GPR waves and have a publication in development. Evaluating whether these data could be used to capture a gradually deforming boundary is a problem that still requires additional evaluation, but could produce a path forward for generalizing our findings to characterizing the soil environment for arbitrary soil conditions.

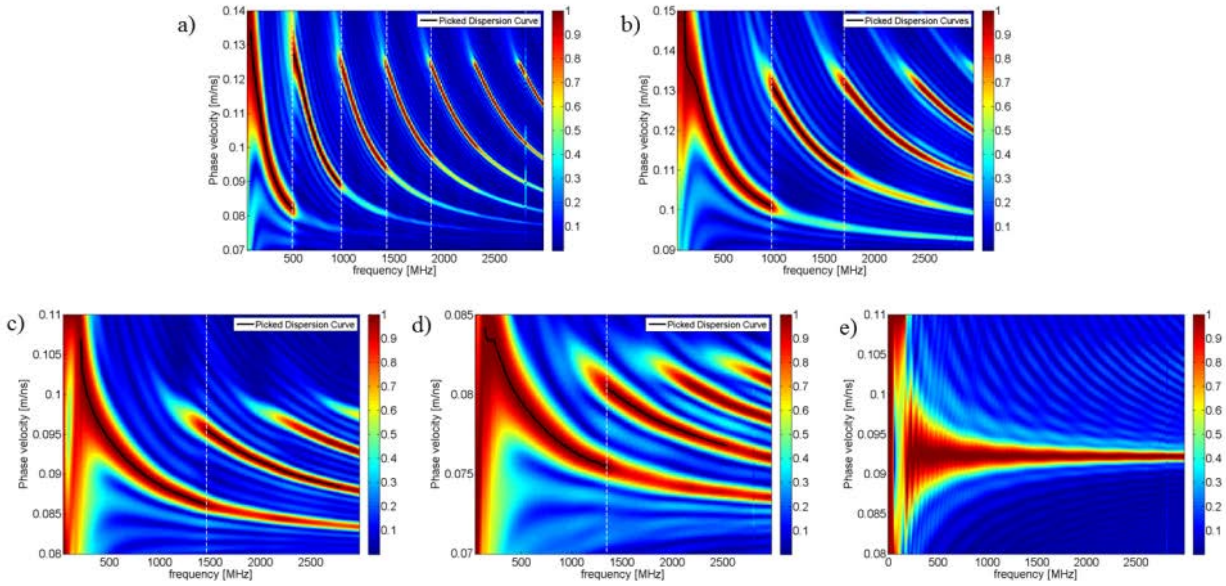

Figure 19: Normalized phase velocity frequency spectra of the GPR simulation results for a) shock front, b) n = 4.0, c) n = 2.1, d) n = 1.5, and e) no waveguide. Vertical dashed white lines indicate cutoff frequencies for dispersive modes and mark the asymptote between modes. The decreasing information contained in these spectra as the waveguide becomes increasingly poorly defined due to stronger capillary effects suggests that characterizing the soil environment.

5. NEURAL NETWORKS AND CLASSIFICATION

An overarching goal of this project is to evaluate whether contextually adaptive pattern recognition algorithms can be developed to account for how changes in the hydrologic state of a soil influence GPR signals. To this end we considered three types of contextual cases for classification systems: (i) a large database of context-dependent signals is used to train the classifier such that hydrologic context is not explicitly considered within the classification system, (ii) GPR signals are corrected to a context-independent reference state prior to classification, and (iii) GPR signals are pre-processed with a general feature extraction neural network prior to classification with a contextual classifier. Prior to evaluating these schemes, we first evaluated the efficacy of using a feed-forward neural network as a forward model for simulating radar responses given that the ability of a network to capture the physics of radar responses influences its ability to transform signals between reference states.

5.1 Neural Networks as a Forward Model

We evaluated feed-forward artificial neural networks (ANNs) to serve as fast, reliable, adaptive forward models for simulating one-dimensional GPR responses. Our most recent version of the network utilizes a vector of dielectric permittivity as input and produces a zero-offset trace of GPR data. A large set of training data was generated by simulating materials with a high permittivity layer located at a random depth. These permittivity profiles were then used to simulate the GPR response of the training data using a numerical GPR forward model (Irving and Knight, 2006) which solves Maxwell's equations in 2D. The network consists of 4600 nodes distributed between three hidden layers and one output layer.

We observed that one problem is that the network tended to produce unrealistic small amplitude events, i.e., noise (Figure 20-21). This is partially due to the large relative amplitude of the groundwave controlling the sensitivity of the network to changes in nodal weights, though additional effort in controlling the number and magnitude of weights in the network is also likely to lead to improvements. To remove this high frequency noise (Fig. 21a) we applied a band pass filter to the network output with a pass band of 500 MHz – 1200 MHz. This range was determined by taking the radar frequency (1000 MHz) and noise frequency (>1500 MHz) into consideration. Utilizing the band pass filter, we are able to more closely represent the desired response of the network (Figs. 21b-c). After the filtering, the total error of all presented patterns was 3e-4 with the largest pattern error at 1e-4; however, there is still some noise in the network response that may be resolved by revising the network topology and taking a modeling approach that focuses on pattern adaptation rather than mimicking the numerical model. Despite the fairly simple approach tested here, however, the results shown in Figures 20-21 indicate that there is significant promise for the neural network to act as a GPR simulator.

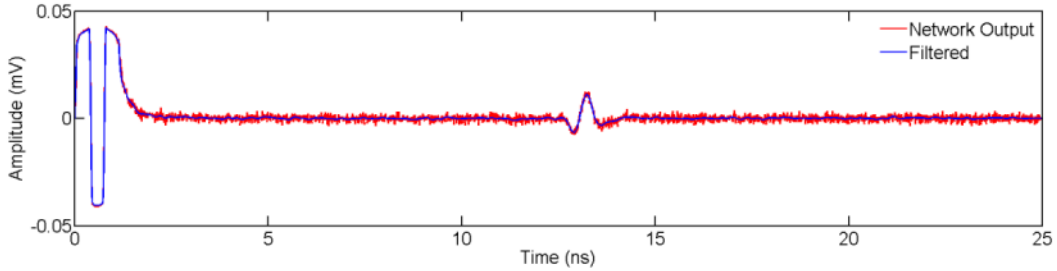

Figure 20: Example of actual and simulated GPR trace obtained from the neural network after filtering.

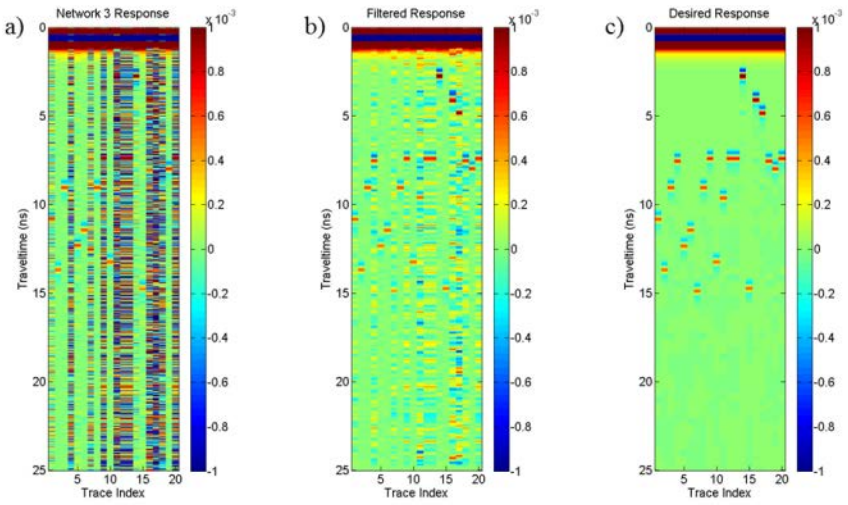

Figure 21: Using a feed forward artificial neural network to determine the radar response of the subsurface using a permittivity vector, a) raw network output, b) band pass filtered network output, c) desired network output, i.e. training data.

5.2 Neural Networks for Target Classification

Target classification can be problematic when using radar data given that the target response varies, sometimes subtly, due to changes in object properties and the surrounding material. One of the largest drivers of this environmental variability in the scope of GPR imaging is volumetric water content. With this work, we look at the capability artificial neural networks to transcend the environmental variability of target response and successfully classify the target from contextual and non-contextual basis.

5.2.1 Network Topologies for Context-Based Classification

We studied three different network topologies for context-based classification to discriminate between mine and clutter objects. In all three cases, the network takes a window of GPR data that has been isolated and extracted from a profile (B scan) after detection by a primary anomaly classifier. The output of the network is the probability that the anomaly is a specific object (e.g., landmine, rock, pipe, etc.).

In the first network topology case (Figure 22a), the network does not explicitly account for the hydrologic state (i.e., water content). In contrast, the second network design first uses water content to correct the GPR signal to a context-independent reference state (i.e., reference water content), which is then passed to a classification network (Figure 22b). The conceptual advantage of this network design is that a limited number of field samples would be required to train the network for a wide range of environmental conditions. The third network topology first acts as a feature extraction step that does not account for hydrologic state. The extracted features are then passed on to a classification network that uses water content as an input to account for hydrologic state (Figure 22c). In all three cases, the overall network topology remains essentially unchanged, except where adding water content as an additional input, though the way information is passed through the network is substantially different.

Figure 22: Network topologies studied as contextual classifiers. In all cases the basic topologic structure of the network remains essentially constant, though the action of the network is significantly different.

a) ***Non-contextual network***: Hydrologic state is not explicitly considered in the network. A large training data set is therefore required to capture the influence of water content variability on GPR signals.

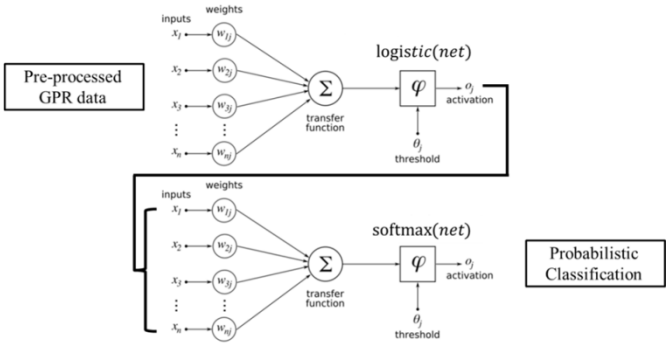

b) ***Corrected to Reference State:*** GPR signals are first corrected to a hydrologic reference state prior to object classification. This approach allows the classification step to remain independent of context.

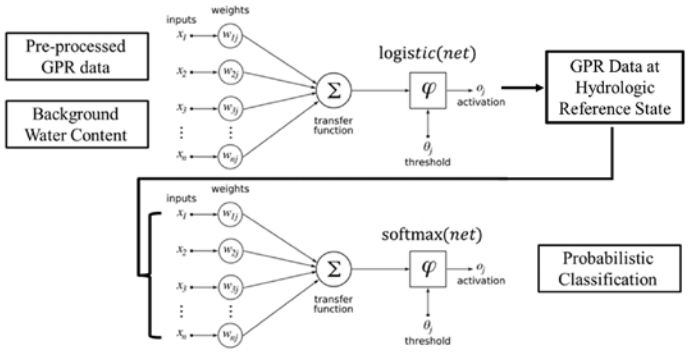

c) ***Contextual Network:*** GPR signals are processed through a feature extraction network to reduce the number of inputs to the classification network. Water content is input as a parameter to the classification network, making this step dependent on hydrologic context.

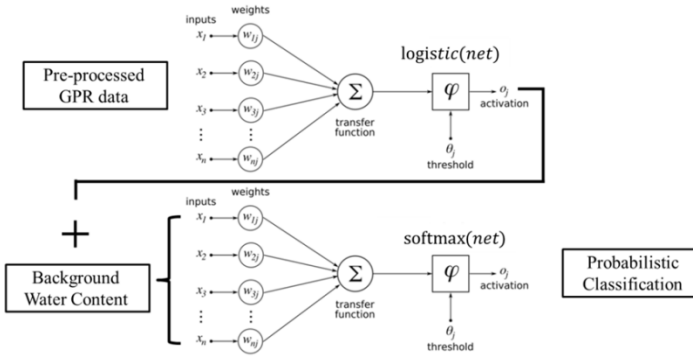

5.2.2 Neural Network Training Data Set

To train the neural network, we developed a simple training set that accounted for changes in object properties and background water content, i.e., a target in a homogeneous background. The data set was constructed using GPR simulations (Irving and Knight, 2006) as these offer a way to develop the large data set that accurately captures the physics of radar required to train a neural network when coupled with our parallel computing capabilities on the Palmetto Cluster. The data set consisted of five targets: 1) an anti-personnel non-metallic cylindrical (APNMC) land mine (Chant et al.,2005), 2) a granitic rock the size of an APNMC mine, 3) a cluster of granitic rocks the size of an APNMC land mine, 4) a metallic pipe (diameter=5cm), and 5) a metallic version of an APNMC landmine (APMC). These targets were inserted at a minimum depth (from top of target to surface) of 5cm into a homogeneous background determined by water content. Water content values from 3-40% were converted to dielectric permittivity using

the Topp equation (Topp, 1980). Magnetic permeability and electrical conductivity were set to be constant as we can expect these to be fairly negligible in most conditions (though these would likely effect wave amplitude and possibly wave velocities at higher values). Examples of how the GPR signal varies between the different objects and water content conditions are given in Figure 23. Portions of this data set were reserved for training, generalization, and validation of the networks. Figure 24 shows the values of water content included in the training data set for each target object. The water content values were selected to create skips and gaps in the water content records appropriate for testing the ability of the neural networks to interpolate and extrapolate to conditions not included in the training data set. The neural networks were trained using the back propagation methods subject to the training data until improvements in the errors obtained for the training data set were balanced by increases in the errors observed for the generalization data set.

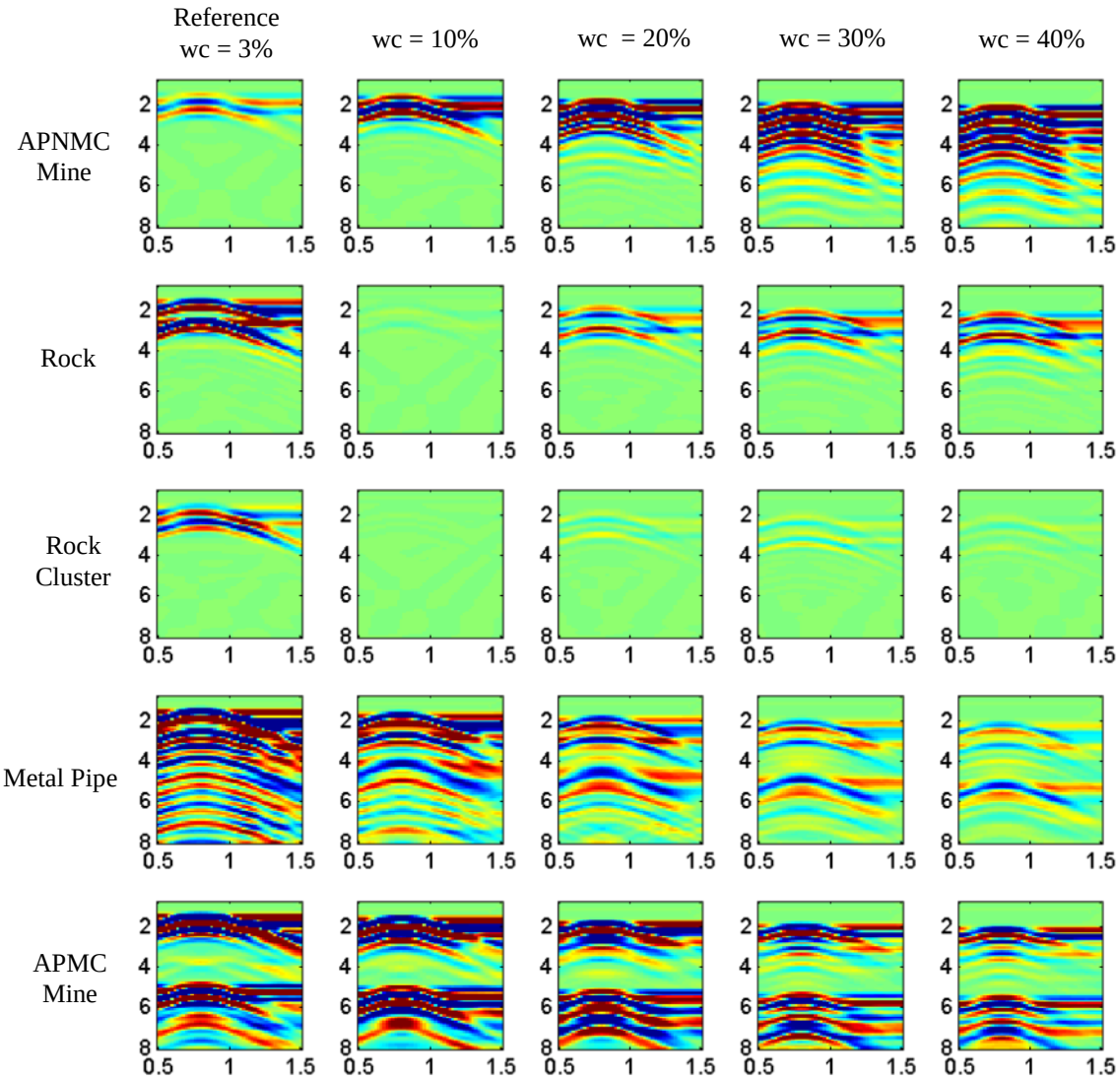

Figure 18: Training data for the network showing the variability in the response of GPR to changes in target and environment. Object variability is seen in the y-direction while representative environment variability is seen in the x-direction. All data have had background subtraction performed.

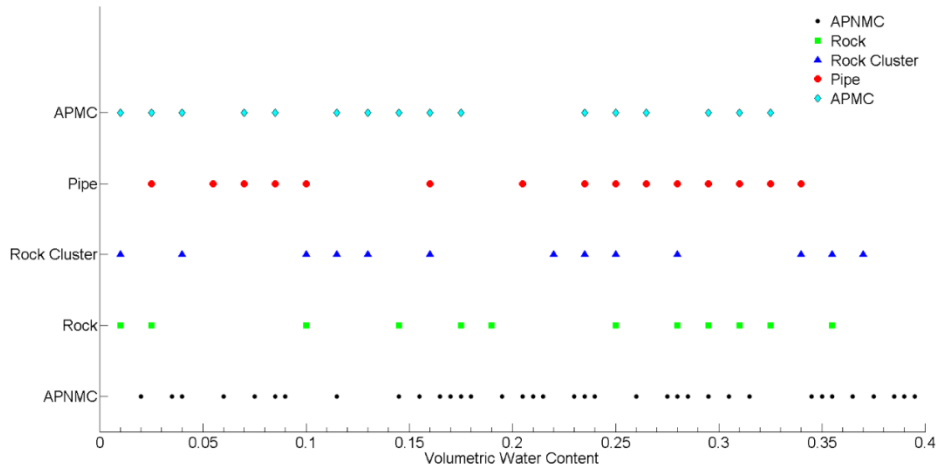

Figure 24: Water content conditions included in the neural network training data sets for various target objects.

5.2.3 Neural Network Validation Data Sets

The purpose of the validation set is to present the neural network with patterns it has never been exposed to during the training procedure to evaluate whether the network is capturing a generalizable functional relationship between inputs and outputs. For these networks, we created four different types of validation sets to test the capabilities of the neural network under different conditions: (i) equilibrium (homogeneous) water content conditions, (ii) equilibrium (non-homogeneous) water content conditions, (iii) a non-equilibrium flow scenario, and (iv) complex clutter scenarios.

The first validation set consisted of GPR responses calculated in a homogeneous water content background, similar to the case for the training data, but at water contents that were excluded from the training data set. This test therefore evaluates the ability of the neural network to interpolate and/or extrapolate patterns between water content values the network has already seen in training.

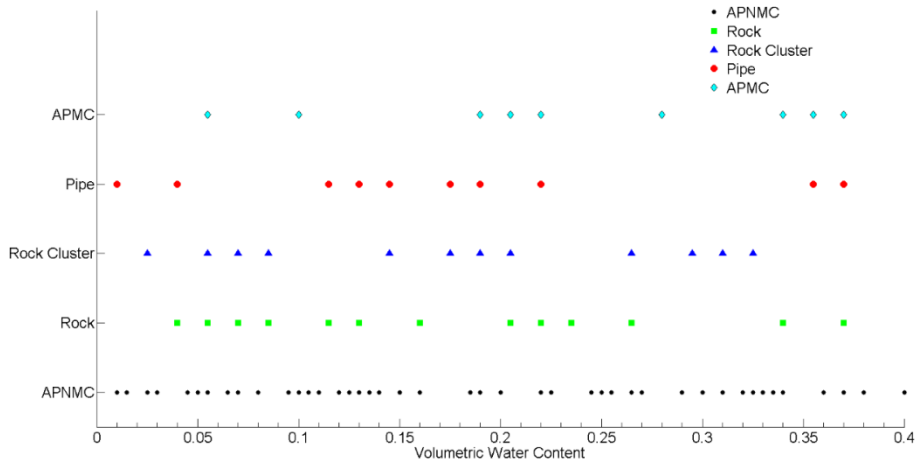

Figure 25: Water content conditions included in the neural network validation data sets for various target objects.

The second validation set is essentially the same as the original training set except that the influence of noise in the data is evaluated by adding variations in the background water content field as random Gaussian perturbations. The network should have a more difficult time with classification of these patterns considering it was trained on homogeneous subsurface simulations. The third validation set represents the time-lapse response of an APNMC mine during infiltration. While this data set is only representative of a single target, the water content values around the mine are complex (Figure 26). This case therefore tests how the network responds to extraneous reflections in the data associated with non-equilibrium hydrologic conditions, as the migrating wetting front produces a reflection on the GPR simulation results separate from that of the mine. The fourth and final validation set tests how the network responds to 1) changes in object size, 2) the placement of objects adjacent to an APNMC mine, 3) unknown and unclassifiable targets (i.e., no class for target), and 4) changes in the orientation of an APNMC mine.

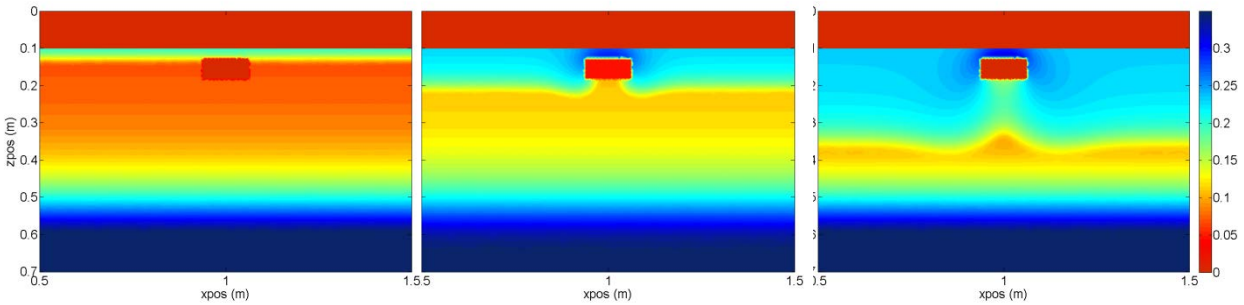

Figure 26: Evolution of the water content field around a landmine during an infiltration event to evaluate the influence of non-equilibrium hydrologic conditions on classification. Results are shown early after the onset of infiltration (left image), while the infiltration front is near the landmine (center image), and after the infiltration front has passed the landmine (right image).

5.2.4 Neural Network Performance in Validation Tests

Trained neural networks with the different topologies described earlier were used to classify targets in each of the validation data sets using GPR data as stimuli. The radar data was preprocessed using background filtering and clipping of the data to reduce the data points in each input pattern to around 3500. For the classification, the networks utilize a modified version of the classic sigmoidal activation function called softmax, which forces the sum of all outputs to unity so they can be interpreted in a probabilistic manner. Using the output of the networks, we can compare their performance using receiver operating characteristic (ROC) curves. These curves describe the performance of classification algorithms and help to determine operating thresholds for maximum performance. Furthermore, the accuracy of a classification algorithm can be quantified by the area under the ROC curve (AUC) (Beran and Oldenburg, 2008).

The results of the first validation test, i.e., where objects were located in soils with homogeneous water content values, are shown in Figure 27. Both contextual and non-contextual networks correctly classify the majority of patterns in the first validation set with AUC values of approximately 0.99, which is considered an excellent classification result. It is emphasized that the non-contextual network was trained on a large set of environmental conditions, thus contained similar information as the contextual network. This is in strong contrast to the case

where the GPR signals were first converted to a reference condition prior to classification, in which case the AUC was substantially lower (0.78), indicating that this approach was not as successful of classification strategy. The successful networks classify the APNMC mine patterns successfully; however, they struggle in classifying a rock vs. a rock cluster. Also, both networks exhibit some confusion when attempting to distinguish a rock cluster from an APNMC and APMC mines at relatively low background water content values (2.5-5.0%), indicating that small reflection amplitudes may pose a problem for the classification algorithms. Considering it is not confusing a target that requires mitigation with one that does not, both networks are viable for further validation tests.

Non-contextual Network

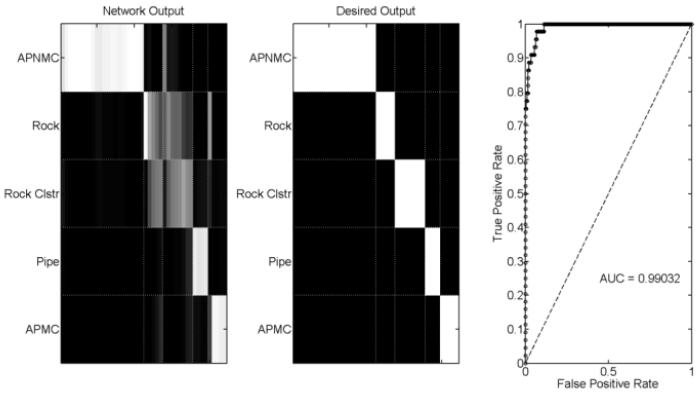

Reference State Corrected Network

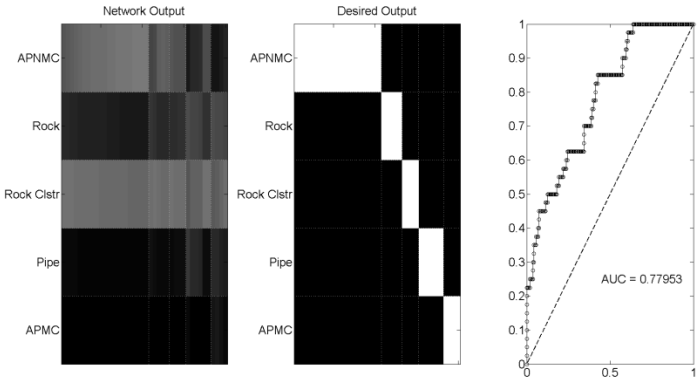

Contextual Network

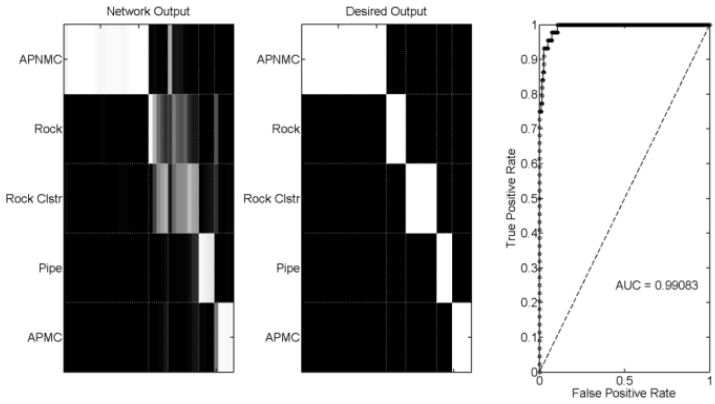

Figure 27: Comparison of classification results for validation test #1 (homogeneous water content). Note that though the non-contextual network performs as well as the contextual network, it was still trained on a wide range of environmental conditions (i.e., water content values), thus illustrating the importance of accounting for hydrologic state.

Non-contextual Network

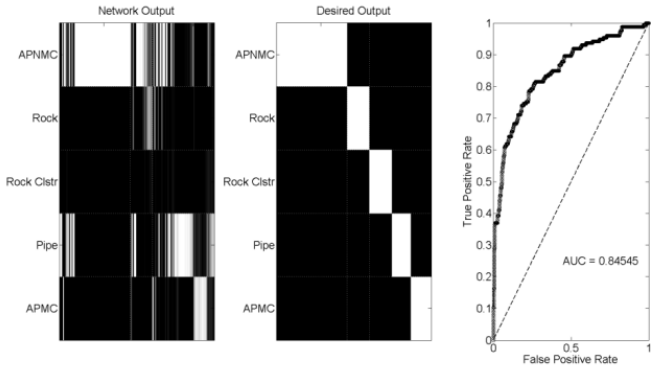

Reference State Corrected Network

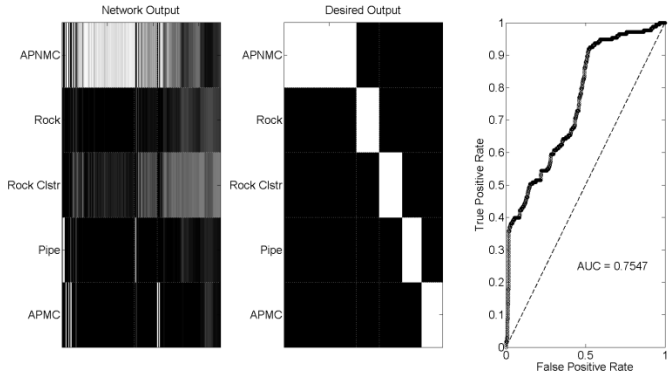

Contextual Network

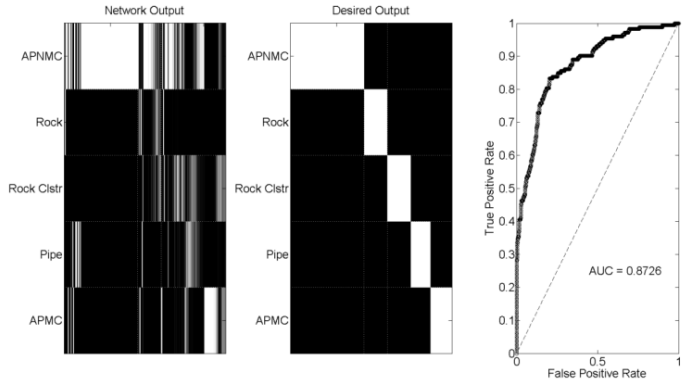

Figure 28: Comparison of classification results for validation test #2 (average uniform water content with random spatial variations).

The second validation test evaluated the impact of spatially variable background water content on the classification results by adding random Gaussian noise to the permittivity matrix of the radar forward model. These simulations are more representative of empirical data collected in the field, as many areas rarely exhibit a homogeneous subsurface in regards to GPR responses. Overall, the networks have a higher level of difficulty in classifying targets, exhibiting much more confusion between the different classes for a given pattern. The non-contextual and contextual networks again show significant performance enhancement (AUC=0.85 and 0.87, respectively) compared to the case where the GPR signal is corrected to a reference state prior to classification (AUC=0.75).

Non-contextual Network

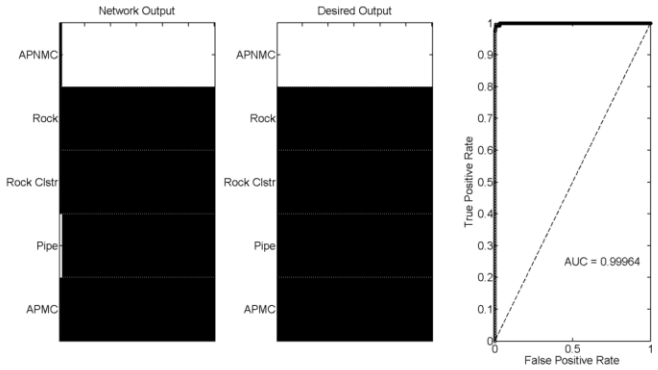

Reference State Corrected Network

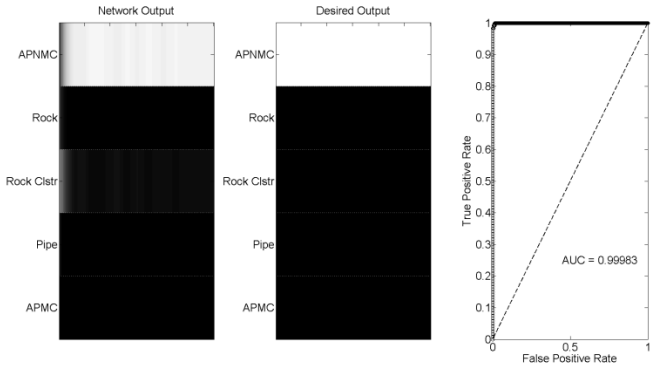

Contextual Network

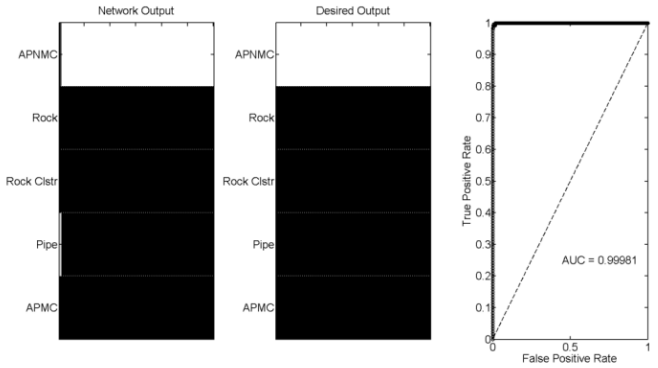

Figure 29: Comparison of classification results for validation test #3 (non-equilibrium water content during an infiltration event). The trial cases represent water content conditions typical of the range of behaviors shown in Figure 26.

The third validation test used the results of a transient infiltration event to represent non-equilibrium distributions of water content. Conditions tested span the range shown in Figure 26 and are representative of non-uniform water contents expected as a result of rainfall and subsequent soil-water redistribution processes. Despite the likely presence of electromagnetic wave dispersion and reflection multiples, the classification results suggest that the networks were all able to perform well except at early times, which affect the near-surface EM wave velocity. This result was unexpected and we are therefore continuing to investigate the influence of non-equilibrium distribution of water contents on landmine classification.

Non-contextual Network

Reference State Corrected Network

Contextual Network

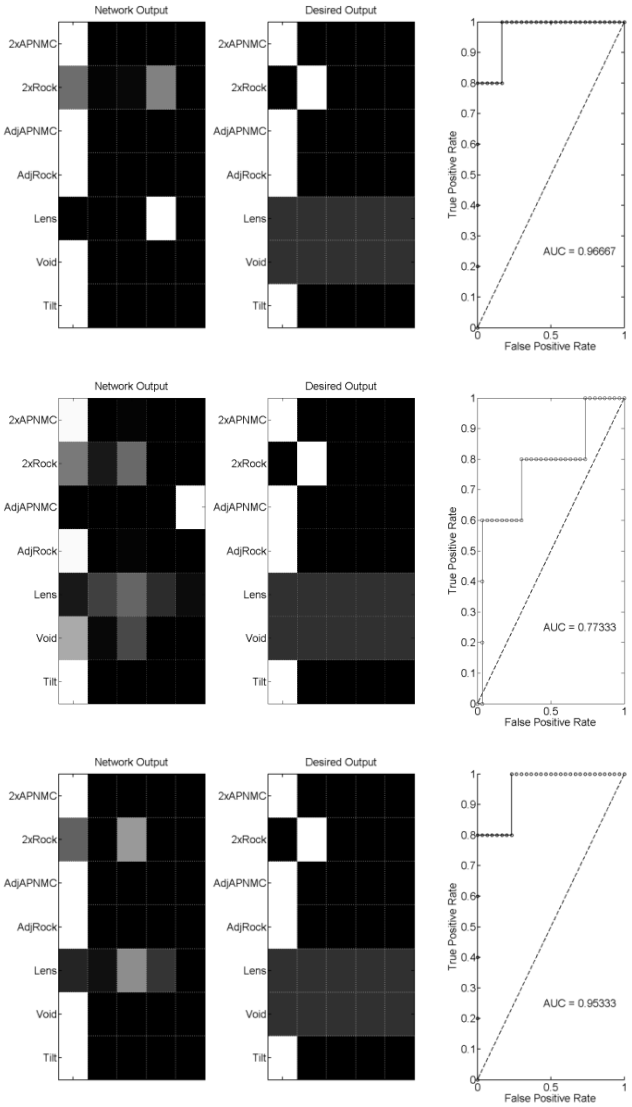

Figure 30: Comparison of classification results for validation test #4 (robust validation set varying target size, adjacency, rotation and including unknown targets).

The final validation test of the neural networks, used a robust test set to evaluate how the network responds to changes in object size, object adjacency, unclassifiable objects, and a non-horizontal target. These test objects are well outside the range of targets used to train the network, so are expected to provide a significant classification challenge. The performance is similar to previous cases, where both the non-contextual and contextual networks perform well compared to the GPR signal correction approach. These networks successfully classify a land mine that is twice the size of the original APNMC mine. The non-contextual network confuses the rock with an APNMC mine and soil lens. The contextual network follows and misclassifies the same target as APNMC mine. Both networks handle object adjacency well given that in the presence of either an adjacent rock or adjacent APNMC mine, the networks are very confident of the target. The same follows for the tilted APNMC mine for both networks. When presented with an unclassifiable target (not in database), however, both networks struggle. Ideally, since the network does not have a class for a soil lens or a void, it should present an equal probability

for all targets. In this respect, the contextual network is a more reliable network in that it presents more confusion when presented with the lens target, indication it may be more applicable to targets outside the original training set.

6. DISCUSSION AND CONCLUSIONS

Our empirical studies and classification tests illustrate that hydrologic state has a substantial impact on GPR signals and our ability to accurately classify targets, like landmines, from these signals. We originally proposed two fundamentally different approaches to adaptive classification of GPR data to account for hydrologic state: 1) hydrologic normalization of GPR data to a reference state prior to classification, and 2) develop of training database that can be tuned to a specific hydrologic state at a particular place and time. A third approach we evaluated was to include hydrologic state data (water content) within a contextual classification algorithm after performing a non-contextual data reduction step on the GPR data. Accounting for hydrologic state within the classification algorithm – either by expanding the training data set to include samples representative of different hydrologic conditions or by explicitly including water content within a contextual network – were found to produce the best classification results. Extracting a unique GPR signature that is independent of the subsurface hydrologic state by correcting GPR signals to a common hydrologic reference state was not found to be an effective approach in this study.

We found that coupling a data reduction and classification step within a contextual network can focus on the influence of contextual data being utilized to improve classification accuracy. The contextual network seems to have a slight advantage over the non-contextual network when presented with patterns absent in the original training data. While other validation sets did not show significant improvement in the accuracy of the network, the contextual network exhibits a modest gain in accuracy when noise is introduced into the GPR data. This same improvement could be expected with empirical data as this is the most representative data set to actual GPR data. Furthermore, there may be a computational advantage for the contextual network as it could lead to a reduced number of nodes in the network topology, faster computational performance, and improved adaptation for unknown conditions given the explicit and more efficient use of hydrologic information.

Finally the high dimensionality of the GPR data was found to play an important role in the performance of the network in training, validation, and deployment phases. Training of the network will take longer with large data sets; however, time from data collection to classification will be minimized as there will be few requirements for preprocessing of the data. Improving implementation of data reduction steps may improve the performance of the network overall, but would require a different network topology and possibly correction of the GPR data, e.g. migration, to account for time shifts in the signals. We therefore conclude that contextual classification algorithms are likely to significantly improve object classification from GPR data, but significant improvements in pre-processing and data reduction could likely further improve these classification results.

References Cited

Berans, L., Oldenburg, D., "Selecting a discrimination algorithm for unexploded ordinance remediation", IEEE Transactions on Geoscience and Remote Sensing, vol. 46, no. 9, 2008.

Chant, I., Lee, D., Ireland,D., "DSTO landmine detection test targets", DSTO Systems Sciences Laboratory, 2005.

Irving J., Knight R., "Numerical modeling of ground-penetrating radar in 2-D using MATLAB," Computers and Geosciences, no. 32, pp 1274-1258, 2006.

Topp G.C., Davis J.L., Annan A.P., "Electromagnetic determination of soil water content: measurements in coaxial transmission lines," Water Resources Research, vol. 16, no. 3, pp. 574-582, 1980.

PUBLICATIONS AND PRESENTATIONS PRODUCED BY THIS PROJECT

Peer reviewed journal articles

Mangel, A.R., S.M. Moysey, J.C. Ryan, and J.A. Tarbutton, "Multi-offset ground-penetrating radar imaging of a lab-scale infiltration test", Hydrology and Earth Systems Science, vol. 16, pp. 4009-4022, doi:10.5194/hess-16-4009-2012, 2012.

Mangel, A.R. S.M. Moysey, and J. van der Kruk, "The effect of capillarity on GPR wave dispersion in precipitation induced waveguides" (complete draft prepared and in editing for submission).

Mangel, A.R., and S.M. Moysey, "Accounting for hydrologic state in GPR classification algorithms" (draft in preparation).

Mangel, A.R., and S.M. Moysey, "Time-lapse 3D imaging of infiltration in soils using GPR" (draft in preparation).

Peer Reviewed Conference Proceedings

Mangel A. R., S.M. Moysey,., A. Creighton, A. Smolka, M. Finley, "Monitoring infiltration in 3D using multi-channel ground-penetrating radar", SEG Expanded Abstracts, accepted for presentation at SEG Annual Fall Meeting, Las Vegas, Nevada, November 2012.

Creighton, A., A. Mangel, and S.M. Moysey, "Three-dimensional time-lapse infiltration monitoring using multi-channel ground penetrating radar", Geological Society of America Abstracts with Programs, Vol. 44, No. 7, p.250, 2012.

Mangel, A.R., S.M. Moysey, J.C. Ryan, J.A. Tarbutton, "Automated multi-offset ground-penetrating radar data collection for monitoring lab-scale infiltration experiments", SEG expanded abstracts, 29, 3774, doi:10.1190/1.3513635, 2010.

Presentations

Mangel, A.R., S.M. Moysey, "The use of contextual data in artificial neural network target classification algorithms for GPR data", 22nd Annual David S. Snipes/Clemson Hydrogeology Symposium, Clemson, SC, April 2014

Mangel, A. R., Moysey, S. M. J., Creighton, A., Song, Y., "Time-lapse 3D GPR imaging of a lab-scale forced infiltration experiment", 21st Annual David S. Snipes/Clemson Hydrogeology Symposium, Clemson, SC, April 2013

Mangel A. R., Moysey, S. M. J., Creighton, A., Smolka, A., Finley, M., "Monitoring infiltration in 3D using multi-channel ground-penetrating radar", Society of Exploration Geophysics Annual Fall Meeting, Las Vegas, Nevada, November 2012.

Mangel, A.R. S.M. Moysey, J. van der Kruk, "Time-lapse GPR WARR surveys during a lab-scale infiltration experiment, SEG-AGU Hydrogeophysics Workshop, Boise, Idaho, July 8-11 2012.

Mangel, A., S.M. Moysey, A. Creighton, A. Smolka, M. Finley, "3D multi-channel GPR imaging of a lab-scale infiltration experiment", Clemson University David Snipes Hydrogeology Symposium, Clemson, South Carolina, 2012.

Mangel A. R., Moysey, S. M. J., "AVO relationships of buried landmine surrogates in variable hydrologic conditions", The Symposium on the Application of Geophysics to Environmental and Engineering Problems (SAGEEP) hosted by The Environmental and Engineering Geophysical Society (EEGS), Tucson, Arizona, March 2012.

Moysey, S.M., "Advances in 3D soil mapping and water content estimation using multi-channel ground-penetrating radar, Abstract H44B-01 presented at 2011 Fall Meeting AGU, San Francisco, CA, Dec. 5-9, 2011, **Invited Talk**.

Mangel, A.R. and S.M. Moysey, "Time-lapse multi-offset imaging of infiltration in heterogeneous media", Abstract H41D-1058 presented at 2011 Fall Meeting AGU, San Francisco, CA, Dec 5-9, 2011.

Moysey, S.M., A. Mangel, "Time-lapse imaging of dynamic systems using multi-offset GPR reflection data", 12th Annual ARO Landmine and UXO Detection Meeting, Washington, D.C., 2011.

Mangel, A., S. Moysey, "Determining transient water content values with ground-penetrating radar reflection surveys", Clemson University David Snipes Hydrogeology Symposium, Clemson, South Carolina, 2011.

Mangel, A.R., and S.M. Moysey, "Time-lapse imaging of dynamic systems using multi-offset GPR reflection data, SAGEEP (Symposium on the Application of Geophysics to Environmental and Engineering Problems), Charleston, SC, April 2011.

Moysey, S.M.J. and A.R. Mangel, “Estimation of soil hydraulic properties using hydrologic trajectories in transient GPR data”, Fall Meeting AGU, San Francisco, CA, Dec. 2010.

Mangel, A.R., S.M. Moysey, J.C. Ryan, J.A. Tarbutton, “Automated multi-offset ground penetrating radar data collection for monitoring lab-scale infiltration experiments”, Annual Meeting SEG, Denver, CO, October 2010.